This pdf file consists of figures and photographs, and their captions, scanned from:

EXAMPLES OF TECTONIC MECHANISMS FOR LOCAL CONTRACTION AND EXHUMATION OF THE LEADING EDGE OF INDIA. SOUTHERN TIBET (28-29 °N; 89-91 °E) AND NANGA PARBAT, PAKISTAN

by

Michael A. Edwards

A Dissertation

Submitted to the University at Albany, State University of New York

in Partial Fulfillment of

the Requirements for the Degree of

Doctor of Philosophy

College of Arts & Sciences

Department of Earth & Atmospheric Sciences

1998

ABSTRACT

In Gonto La valley, southern Tibet, a continuous, planar, ~10°N dipping detachment horizon juxtaposes Tethyan slates over a footwall of leucogranite that intrudes a S-dipping injection complex layer that I regard as a rotated Southern Tibet Detachment System (STDS) horizon. This is deformed & partially cut by the leucogranite which forms a pluton extending throughout Khula Kangri massif. In collaboration, ^{208}Pb-^{232}Th measurements on 12 monazite grains of the leucogranite gave a crystallization age of 12.5±0.4 Ma. Integrated estimates of magnitude, and rate, of detachment displacement suggest that STDS displacement continued after granite crystallisation for 1-3 m.y. Therefore N-S extension in southern Tibet continued into the Late Miocene. A new geologic map of the Khula Kangri and Kanga Punzum-Monlakarchung High Himalayan ranges is presented using field, satellite & topographic data. These define a fork in the High Himalaya that results in a repetition of the main geological section. The STDS can be traced around both ranges and is a continuous surface. A simple model of post detachment, scissor faulting and block rotation is proposed. In SE Nanga Parbat Haramosh Massif (NPHM), Pakistan, field and microstructural analysis of strain and sense of shear trends indicate that several km of metasedimentary schists and gneisses are Himalayan Main Mantle Thrust (MMT) footwall rocks rotated to vertical due to NW-SE directed shortening. Near the NPHM summit region, several km of non-coaxially sheared granitic orthogneiss show W over E displacement structures. Although deformation mechanisms appear lower temperature than in the MMT footwall rocks, a major "uplift" structure (the Rupal Chichi shear zone - RCSZ) is proposed. To the SW, an E-over W shear zone (the Diamir Shear Zone - DSZ) that coincides with a syn-kinematically intruded granite (the Jalhari Granite) is recognised. In collaboration, ^{208}Pb-^{232}Th measurements on monazite grains of the Jalhari indicate displacement has continued from ~9 to <3 Ma. The DSZ is regarded as the mechanical continuation of the Raikot Fault. The Raikot-DSZ, together with the RCSZ define a conjugate pair that is interpreted to mark a pop-up structure, allowing the skywards displacement of NPHM.

TABLE OF CONTENTS

LIST OF FIGURES

Page

CHAPTER TWO

LIST OF TABLES

Page

Figure 2.1

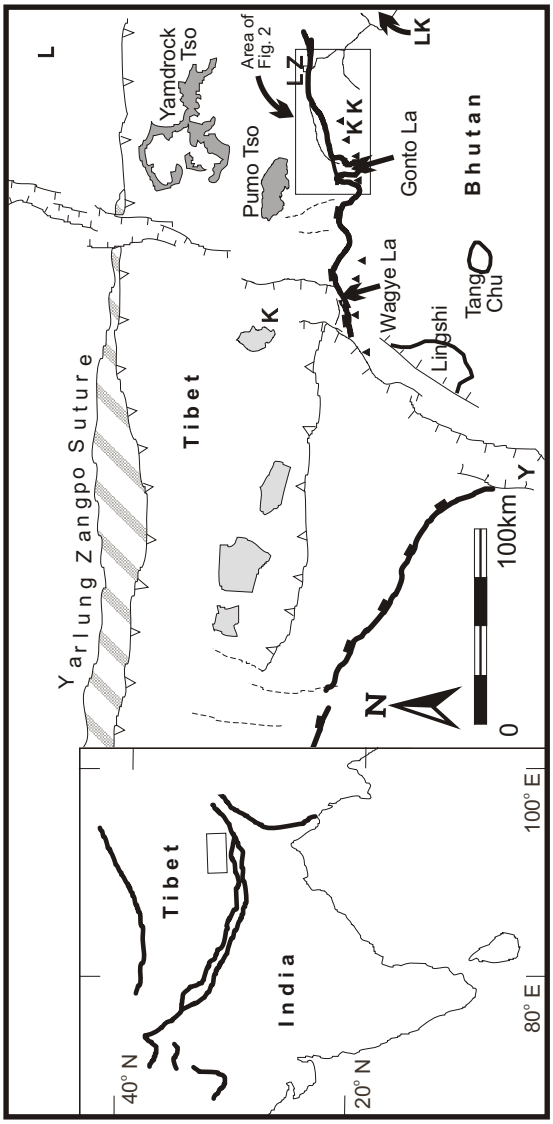

Figure 2.1 Map showing main geological features of Southern Tibet. Stripes: Zangpo suture ophiolites and sediments of Xigaze Group; light grey: leucogranites of Lhagoi-Kangri belt; dark grey: lakes; lines with single barbs: Quaternary normal faults; lines with triangular barbs: thrusts; heavy lines with boxes: approximate trace of STDS; KK, Khula Kangri massif; LZ, Lhozag; LK, La Kang. Inset shows regional location of map area (box) in which thick black lines are major tectonic discontinuities. Modified after Burg et al. (1984). [L - Lhasa; K - Kangmar; Y - Yadong]

Figure 2.2

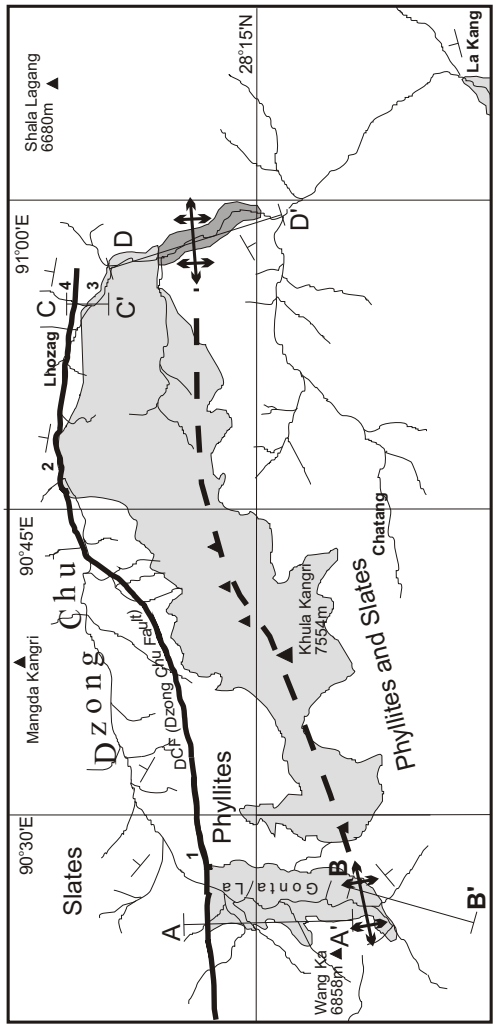

Figure 2.2 Geologic summary map of Khula Kangri area (box in fig. 2.1). Light grey: Khula Kangri leucogranite pluton; dark grey: High Himalayan Crystallines structural window to High Himalayan crystalline series; black triangles: peaks over 6500m; dashed black line: approximate trace of regional antiform; numbers: locations referred to in text. Tethyan sequences named in their approximate location. Cross section locations are shown. Some high peaks are capped by slate and phyllite (not shown).

Figure 2.3

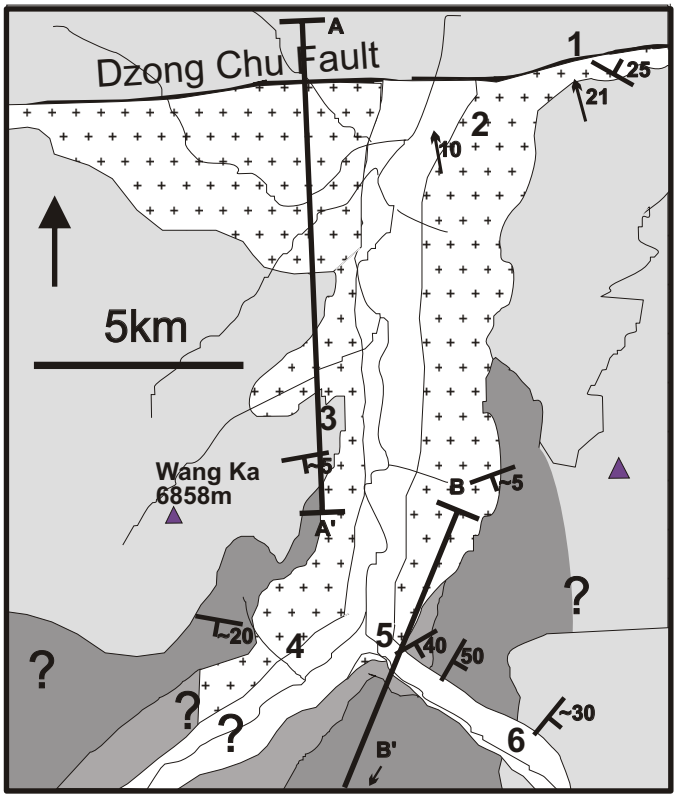

Figure 2.3 Geologic map of Gonto La valley (box in fig. 2.2). Crosses: leucogranite; light grey: Tethyan Mesozoic marble and phyllite; dark grey: injection complex; medium grey: gneiss; white: Quaternary cover and slates north of Dzong Chu fault. Numbers are locations referred to in text. Strike and dip symbols refer to foliation, arrows are lineation measurements (remote measurements are given as approximate dips). Question marks indicate specific uncertainty. A-A' and B-B' are cross section lines.

Figure 2.4

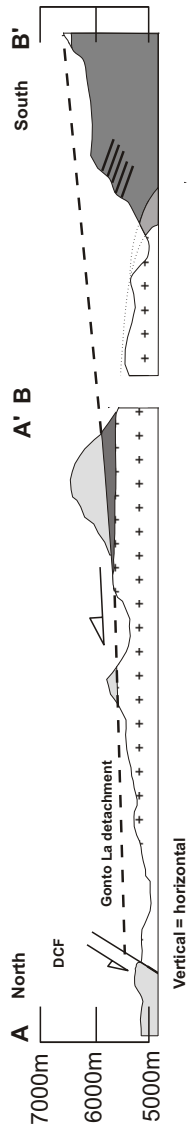

Figure 2.4 Cross Section A-A' and B-B' along Gonto La valley (located on fig. 2.3). Section A-A' is along western side of Gonto La valley, projected on to east facing line. Gap in section indicates join of two sections. Lines on south wall represent foliation within injection complex .Small unshaded area in south is snow line on north shoulder of Kanga Punzum. Shading as for fig. 2.3.

Figure 2.5a

Figure 2.5a see caption on next page

Figure 2.5b

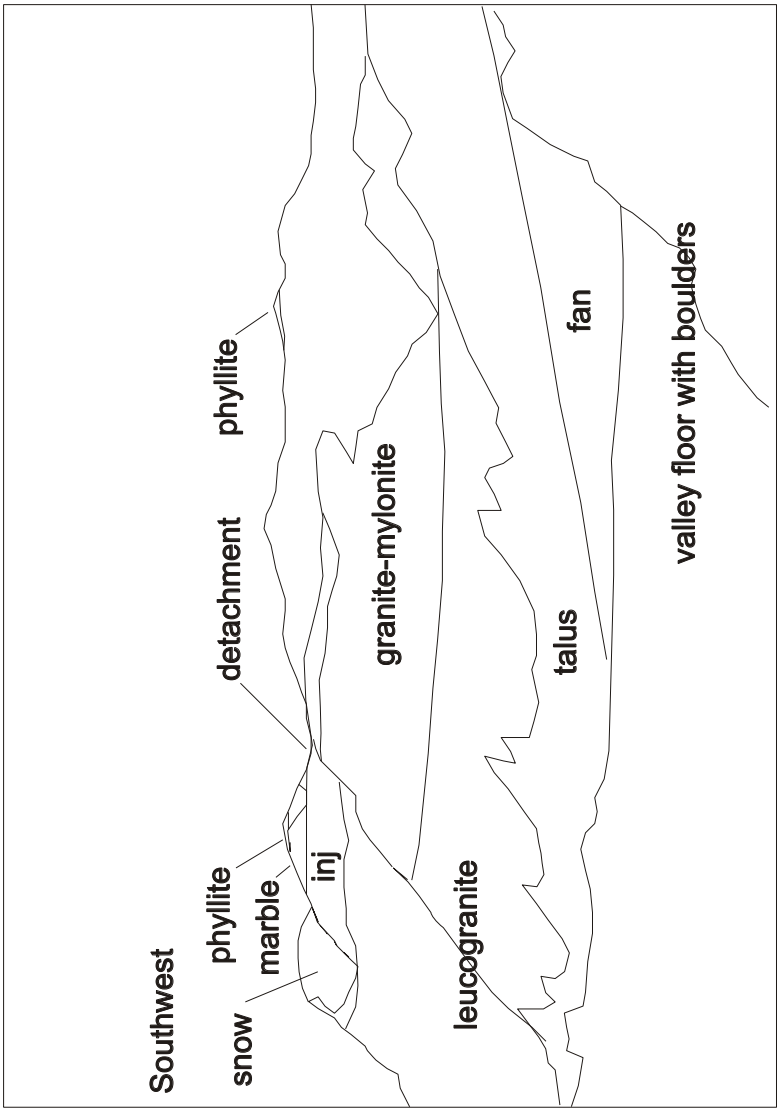

Figure 2.5b [a (previous page) & b] Photo and line drawing looking WSW from location 1 (fig. 2.3) at N end of Gonto La valley. Gonta La detachment is continuous line running across hillside, dipping approximately 10°N. Upper 300m up to detachment is granite-mylonite. Jagged cliffs in foreground are leucogranite of Khula Kangri pluton. Light and dark horizontal bands on peaks above detachment are gently north-dipping sequences of marble and phyllite respectively (described in text). Note thin outcrop of gently south dipping injection complex (inj) at location 3 (fig. 2.3), which illustrates gradual excision by both Gonto La detachment above, and pluton below. Towards south, injection complex layer systematically increases in both thickness and angle of dip (see description in text). DCF outcrops to right, outside field of view.

Figure 2.6a

Figure 2.6a see caption on next page

Figure 2.6b

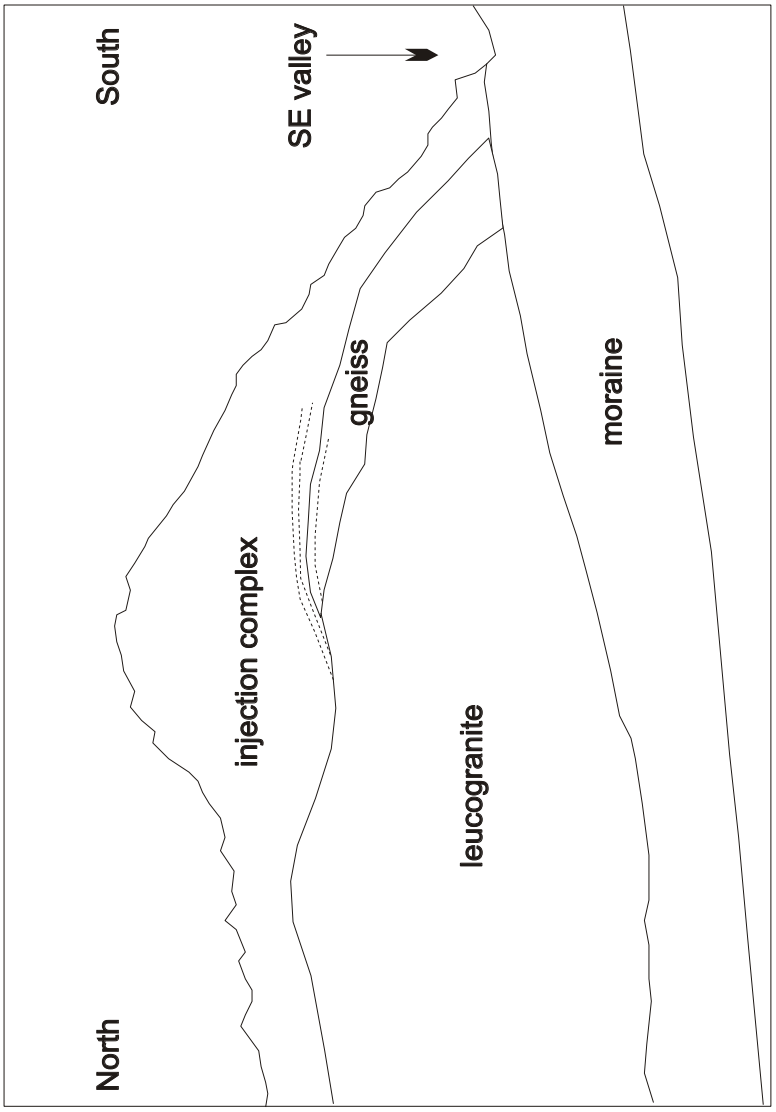

Figure 2.6b [a (previous page) & b] Photo and line drawing from location 4 (fig. 2.3) ~200m above valley floor on SW corner of main Gonto La valley looking across to entrance to SE valley (location 5, fig. 2.3). View shows intrusive southern contact of leucogranite of Khula Kangri pluton truncating the gneiss and, to left, cutting leucogranite sills which define macroscopic foliation. The leucogranite is unfoliated at this contact. This cross-cutting relationship requires that the granite post-dates development of the mylonite of the injection complex (see text). Mesozoic (?) phyllites, structurally above the injection complex, outcrop up the SE valley, out of view. The Gonto La detachment projects from where it last outcrops to the north (left) to above present erosion level. Apparent antiformal shape of foliation (dashed lines on line drawing) is distortion due to perspective.

Figure 2.7

Figure 2.7 Photomicrograph of mylonitic horizon of leucogranite (appendix B) from location 2 (fig. 2.3) in northern Gonto La valley illustrating typical sense of shear indicators observed. Cut perpendicular to foliation, parallel to lineation (350°); crossed polars. Side of image is ~4.0mm. North is to base, south to top. Polycrystalline quartz and feldspar ribbon aggregates define S-surfaces. In lower centre, asymmetry of inclusion tails of feldspar grain and mica fish show sinistral sense of shear (top-to-north).

Figure 2.8

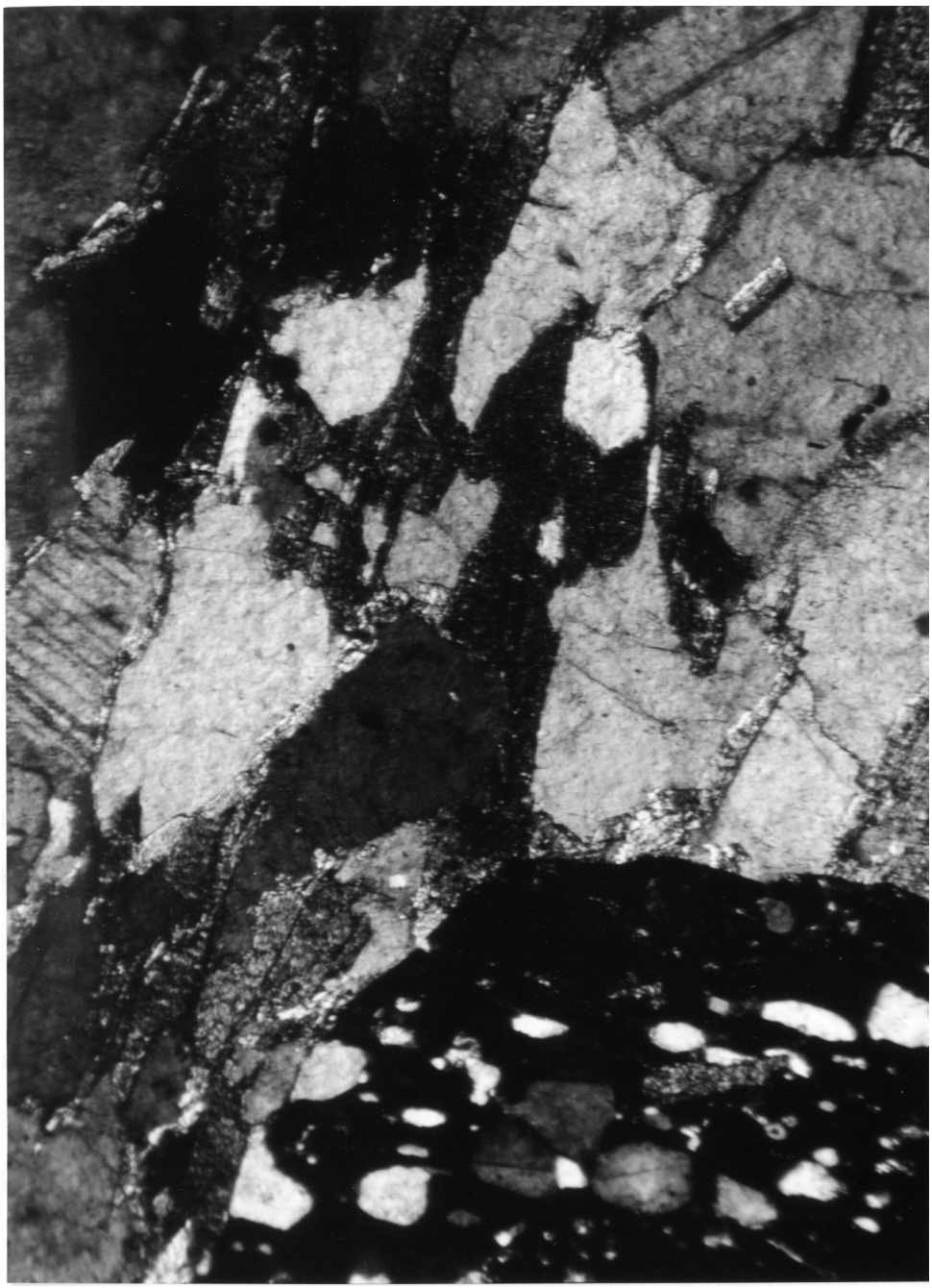

Figure 2.8 Photomicrograph of biotite-sillimanite gneiss (appendix B) near intrusive contact in southern Gonto La valley (location 5, fig. 2.3). Side of image is ~4.0mm. S_1 (in garnet grain) shows a foliation at a high angle to S_2, the gneissic foliation. Crossed polars.

Figure 2.9

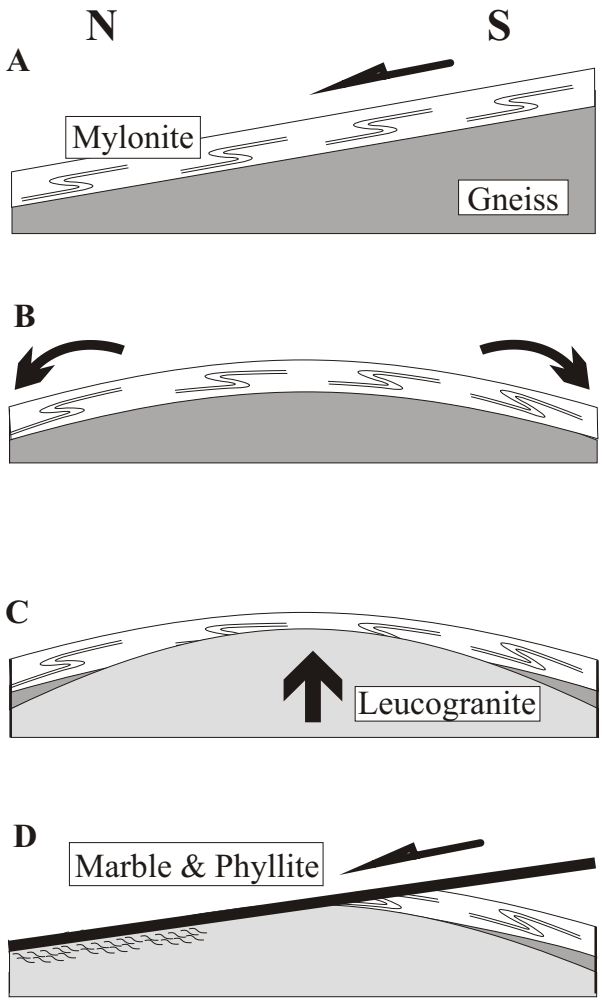

Figure 2.9 Schematic illustration of interpreted history of Gonto La area. A: early N-S extension develops thick mylonitic injection complex horizon; a ductile, normal sense shear zone above gneiss (asymmetric fold symbols are general represention of sense of shear indicators found). B: folding or other mechanism causes rotation of southern part of mylonitic horizon to S-dipping (possibly associated with leucogranite intrusion, see discussion in text). C: Emplacement of Khula Kangri pluton truncates foliation of gneiss and injection complex. D: later N-S extension causes further normal faulting (the observed Gonto La detachment) juxtaposing Mesozoic slate over leucogranite, gneisses, and injection complex. The implied hiatus in N-S extension is not required; displacement may have transferred to a structurally higher level before pluton emplacement.

Figure 2.10

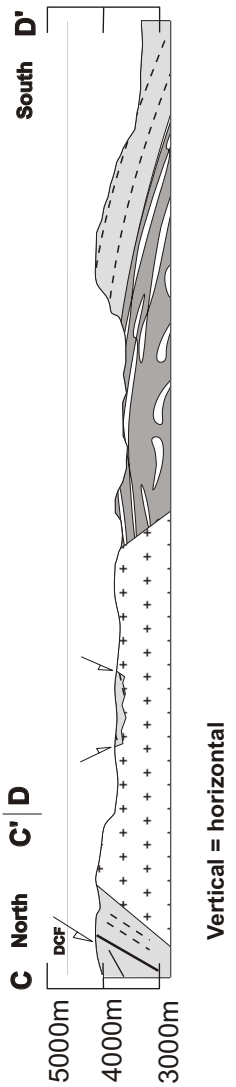

Figure 2.10 Cross section C-C' and D-D' from Lhozag to the Chatang valley confluence point, ~15km north of La Kang (located on fig. 2.2). Shows antiformal culmination with HHC exposed in central portions Light grey: Mesozoic slate (ornament indicates foliation); crosses: leucogranite; dark grey: general HHC (ornament showing shematic augen represents quartzofeldspathic augen gneiss and marbles; lens-shaped ornament is injection complex above); Injection complex is thought to be the location for the extensional horizon on which the Palaeozoic is excised.

Figure 2.11

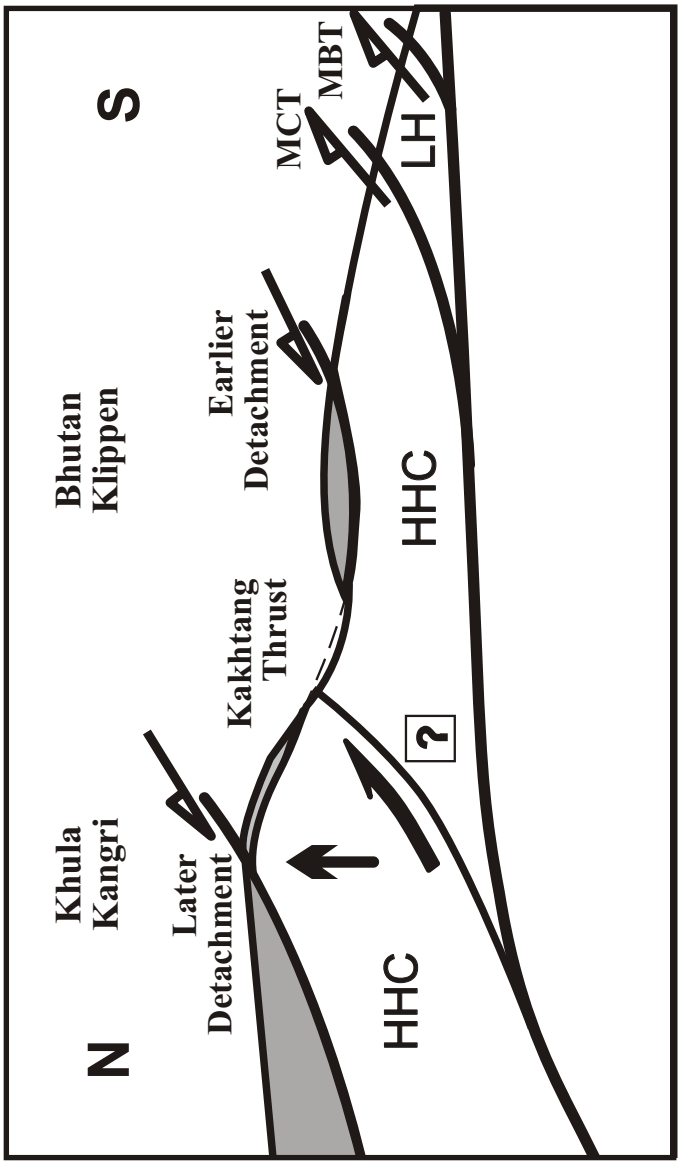

Figure 2.11 Cartoon crustal section to show hypothesis of large scale relationship between early and late detachments in southern Tibet and Bhutan. Grey shade: Tethyan sedimentary sequences; HHC, High Himalayan crystalline series; LH, Lesser Himalayan sequences; heavy lines: faults. Half-arrows show direction of relative offset of hanging wall. Large half arrow and full arrow represent general mechanism of rise of magma and uplift relative to lower Bhutan. Kakhtang thrust is suggestively added as one of the possibilities for a general magma pathway, relative uplift and folding of earlier STDS horizon(s) (see discussion in text). Footwall and hanging wall thicknesses are not intended to be accurate representations.

Figure 3.1A

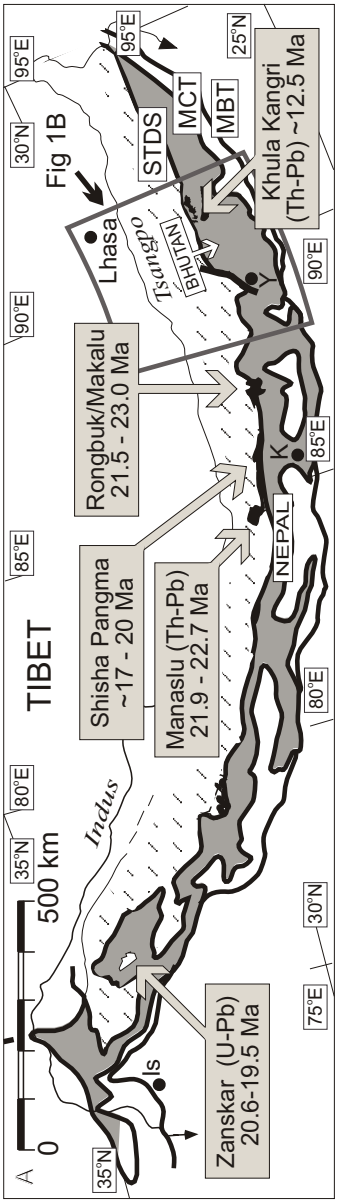

Figure 3.1A Tectonic map of Himalaya (after Gansser, 1983; Pêcher, 1991). White: Lesser Himalayan sequences. Grey: Greater Himalayan crystalline sequence. White with dashed hatch: Tethyan sedimentary sequence. Black areas adjacent to arrows: high Himalayan granite plutons. Boxes with arrows locate specific crystallization ages of granites (from west to east, sources are: Noble and Searle, 1995; Harrison et al., 1995b; Searle et al., 1997; Harrison et al., 1995b; this study). STDS is southern Tibet detachment system; MCT is main central thrust; MBT is main boundary thrust.

Figure 3.1B

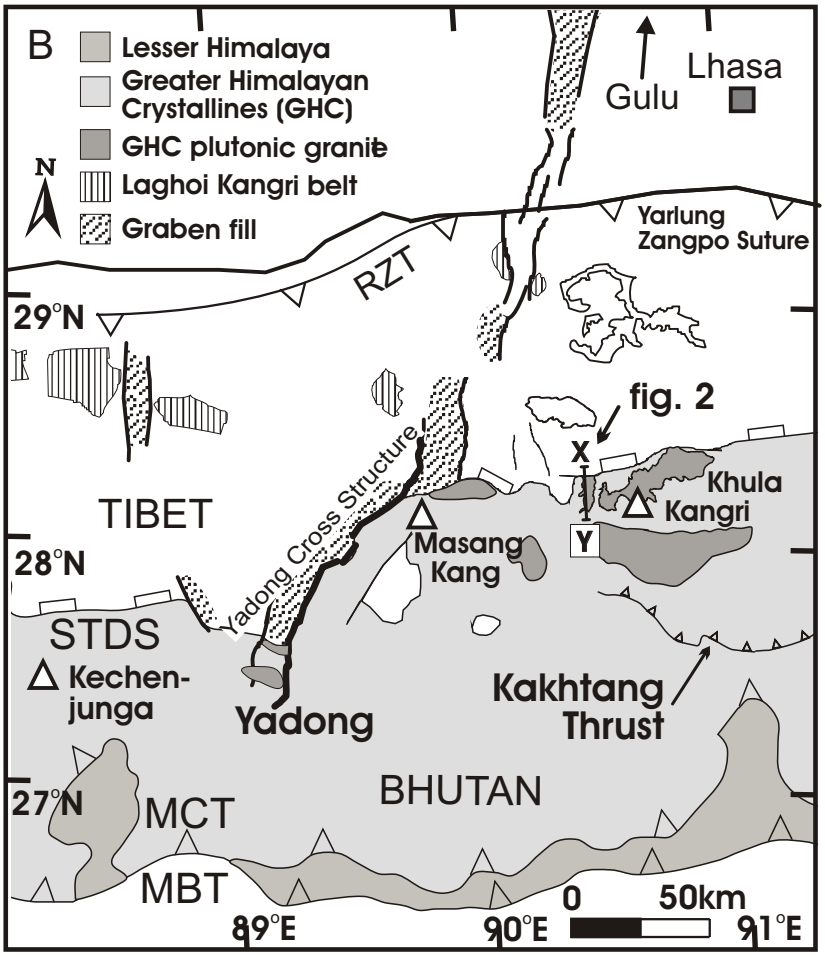

Figure 3.1B Tectonic map of area around southern Yadong-Gulu rift system (after Gansser, 1983; Burg, 1983; Burchfiel et al., 1992; Edwards et al., 1996). White (between STDS and suture): Tethyan sedimentary sequence. Heavy north - south trending lines: normal faults due to east - west extension. White triangles: major peaks. Yadong Cross structure is represented by ~70 km offset of high peaks and trace of STDS. Gulu, (at north end of Yadong - Gulu rift) is ~100 km north - northeast of arrow.

Figure 3.2

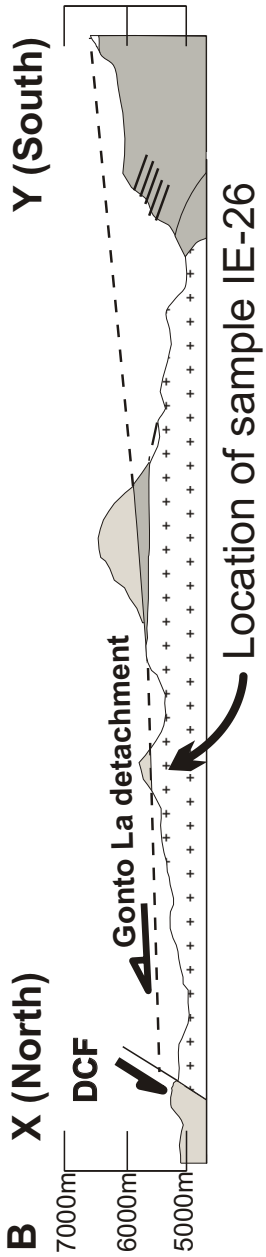

Figure 3.2 Generalized cross section (x-y) through Gonto La valley. Plus pattern is Khula Kangri granite. Darker shading is general Greater Himalayan crystalline sequence. Lighter shading above detachment is Tethyan sedimentary sequence. DCF is Dzong Chu normal fault. Location of sample IE-26 is immediately below ~300 m - thick granite-mylonite horizon which is below Gonto La detachment. Half - arrows show relative movement direction of fault hanging walls. After Edwards et al. (1996).

Figure 3.3

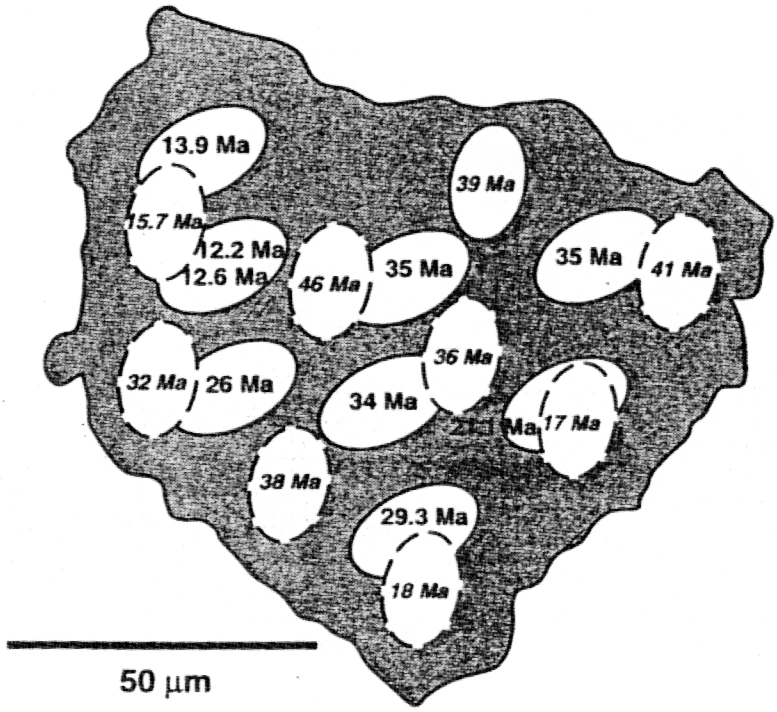

Figure 3.3 Map of monazite grain c, sample IE-26, showing locations and ages of individual ion microprobe analysis spots. Results from first and second analysis set are respectively shown as solid and dashed ellipses. Note proximity between oldest (46 Ma) and youngest (12 Ma) results (see text). Because old core likely represents Eo-Himalayan metamorphism and youngest age represents time of anatexis, lack of equilibration over ~10 μm distance restricts time at peak temperature to no more than ~1 m.y.

Table 3.1

analysis	$^{204}Pb/^{206}Pb$	σ	$^{208}Pb/^{232}Th$	σ	$^{232}ThO_2/Th$	σ	$frac_{com\ Pb}$	σ	Age (Ma)	± (Ma)
asp1	0.00166	0.00001	0.0309	0.00004	5.88	0.0025	0.066	0.0005	13.2	0.4
asp2	0.00169	0.00001	0.0309	0.00002	5.90	0.0035	0.067	0.0004	13.1	0.4
bsp1	0.00222	0.00003	0.0286	0.00003	5.79	0.0017	0.088	0.0011	12.3	0.4
csp1	0.00113	0.00001	0.0737	0.00004	5.62	0.0021	0.045	0.0005	34.1	0.7
dsp1	0.00344	0.00013	0.0212	0.00004	4.70	0.0102	0.137	0.0051	11.0	0.7
csp2	0.00343	0.00006	0.0299	0.00017	5.66	0.0060	0.136	0.0025	12.6	0.6
csp3	0.00109	0.00003	0.0699	0.00010	5.29	0.0043	0.044	0.0013	34.9	0.6
csp4	0.00206	0.00008	0.0566	0.00083	5.00	0.0928	0.082	0.0032	29.3	1.0
csp5	0.00131	0.00005	0.0333	0.00013	3.70	0.0067	0.052	0.0020	25.9	0.6
csp6	0.00128	0.00003	0.0432	0.00011	3.60	0.0055	0.051	0.0010	35.2	0.6
csp7	0.00690	0.00010	0.0229	0.00024	3.65	0.0089	0.275	0.0041	13.9	2.1
csp8	0.00179	0.00008	0.0372	0.00008	4.62	0.0059	0.071	0.0033	21.1	0.6
csp2@1	0.00193	0.00015	0.0089	0.00006	2.40	0.0058	0.077	0.0061	12.2	0.3
esp1	0.00418	0.00016	0.0211	0.00006	4.85	0.0033	0.166	0.0064	10.1	0.6
esp2	0.00441	0.00008	0.0256	0.00005	5.33	0.0058	0.175	0.0032	10.9	0.7
fsp1	0.00517	0.00041	0.0251	0.00004	5.07	0.0122	0.206	0.0163	10.5	0.3
gsp1	0.00713	0.00023	0.0359	0.00030	6.70	0.0238	0.284	0.0080	10.1	0.9
gsp2	0.00828	0.00062	0.0364	0.00029	6.69	0.0036	0.330	0.0245	10.0	0.7
asp3	0.00538	0.00018	0.0369	0.00010	6.41	0.0068	0.214	0.0062	12.4	1.0
fsp2	0.00339	0.00009	0.0203	0.00003	4.11	0.0023	0.135	0.0034	12.8	0.4
gsp3	0.00131	0.00003	0.0255	0.00006	5.36	0.0073	0.052	0.0011	12.7	0.3
hsp1	0.00506	0.00043	0.0347	0.00178	5.97	0.0040	0.201	0.0172	12.5	0.6
hsp2	0.00278	0.00015	0.0367	0.00008	6.53	0.0081	0.111	0.0061	13.2	0.4
isp1	0.00235	0.00015	0.0273	0.00008	5.54	0.0042	0.093	0.0060	11.9	0.3
isp2	0.00436	0.00023	0.0284	0.00010	5.66	0.0080	0.173	0.0092	11.3	0.5
jsp1	0.00183	0.00017	0.0233	0.00005	4.77	0.0029	0.073	0.0068	12.7	0.2
lsp3	0.00248	0.00044	0.0259	0.00005	5.45	0.0042	0.099	0.0175	11.7	0.5
ksp1	0.00228	0.00014	0.0382	0.00008	6.75	0.0084	0.091	0.0056	13.6	0.2
ksp2	0.00239	0.00009	0.0348	0.00009	6.48	0.0034	0.095	0.0036	13.0	0.3
lsp1	0.00255	0.00012	0.0322	0.00007	6.03	0.0012	0.102	0.0381	12.9	0.5
lsp2	0.00156	0.00006	0.0212	0.00002	4.44	0.0043	0.062	0.0024	12.7	0.3
jsp2	0.00184	0.00004	0.0277	0.00002	5.73	0.0050	0.073	0.0015	12.3	0.3
jsp3	0.00156	0.00006	0.0264	0.00005	5.49	0.0023	0.062	0.0025	12.3	0.3
jsp3@1	0.00200	0.00005	0.0220	0.00011	4.65	0.0132	0.080	0.0022	12.4	0.4
lsp3	0.00154	0.00128	0.0160	0.00004	3.76	0.0033	0.061	0.0511	12.0	0.3

Table 3.1 Th-Pb monazite results for sample IE-26 (12 monazite grains "a" to "l").

Figure 4.1

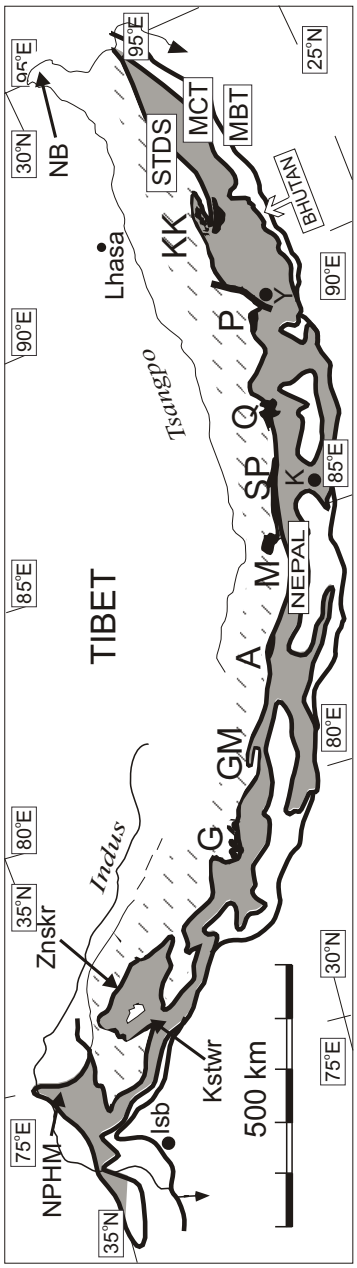

Figure 4.1 General geologic map of Himalayan chain. Light grey: Higher Himalaya Crystalline sequence (HHC). White with broken hatch pattern: Tethyan sedimentary sequence. White: Lesser Himalayan sequences (where part of MCT footwall). Black blobs: High Himalayan granite plutons; letters are associated high peaks [Ga; Gangotri, GM; Ghurla Mandhata, A; Annapurna, M; Manaslu, SP; Shisha Pangma, Q; Mt. Everest, P; Pauhunri, KK; Khula Kangri]. NPHM: Nanga Parbat Haramosh Massif, Isb: Islamabad, Kstwr: Kishtwar window, Znskr: Zanskar, K: Kathmandu, Y: Yadong, NB: Namche Barwah. STDS: Southern Tibet Detachment System. MCT: Main Central Thrust. MBT: Main Boundary Thrust

Figure 4.2

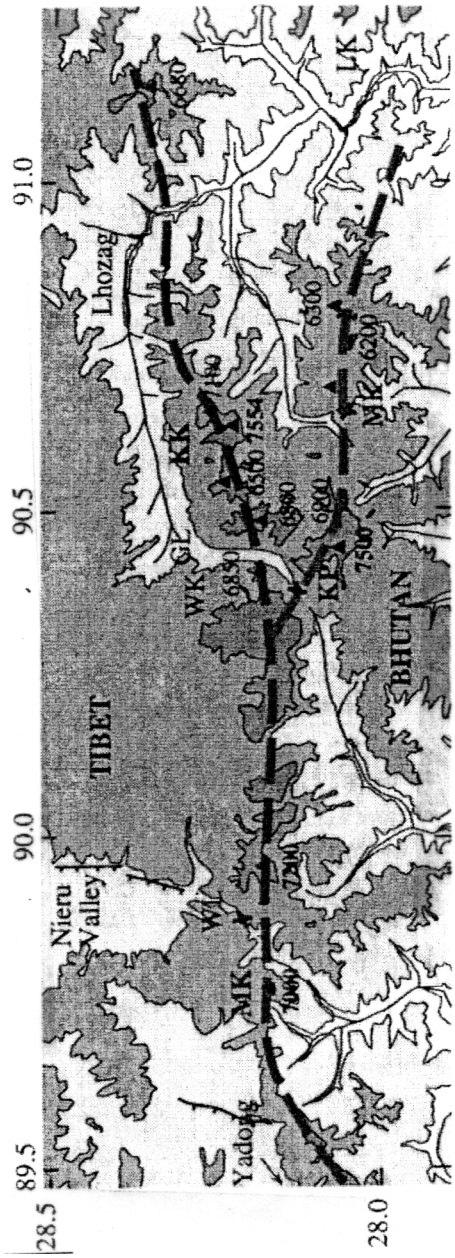

Figure 4.2 Regional topographic map of Tibet-Bhutan frontier area Himalaya immediately east of Yadong-Gulu rift system. Numbers are degrees east (89.5, etc), or north (28.0, etc.). Contour interval: 1000m; darkest shading is >6000 m (>7000m not discriminated). Fine dashed lines are approximate trace of main rivers. Thick line is approximate line of high peaks. Selective peaks and passes are shown: WL; Wagye La, MgK; Masang Kang, WK; Wang Ka, GL; Gonto La, KK; Khula Kangri, KP; Kanga Punzum, MK Monlakarchung La, LK; La Kang. Note bifurcation in line of high topography (High Himalaya) is co-incident with repetition of main High Himalaya geologic sequence. Khula Kangri range is north fork, Kanga Punzum-Monlakarchung range is south fork.

Figure 4.3

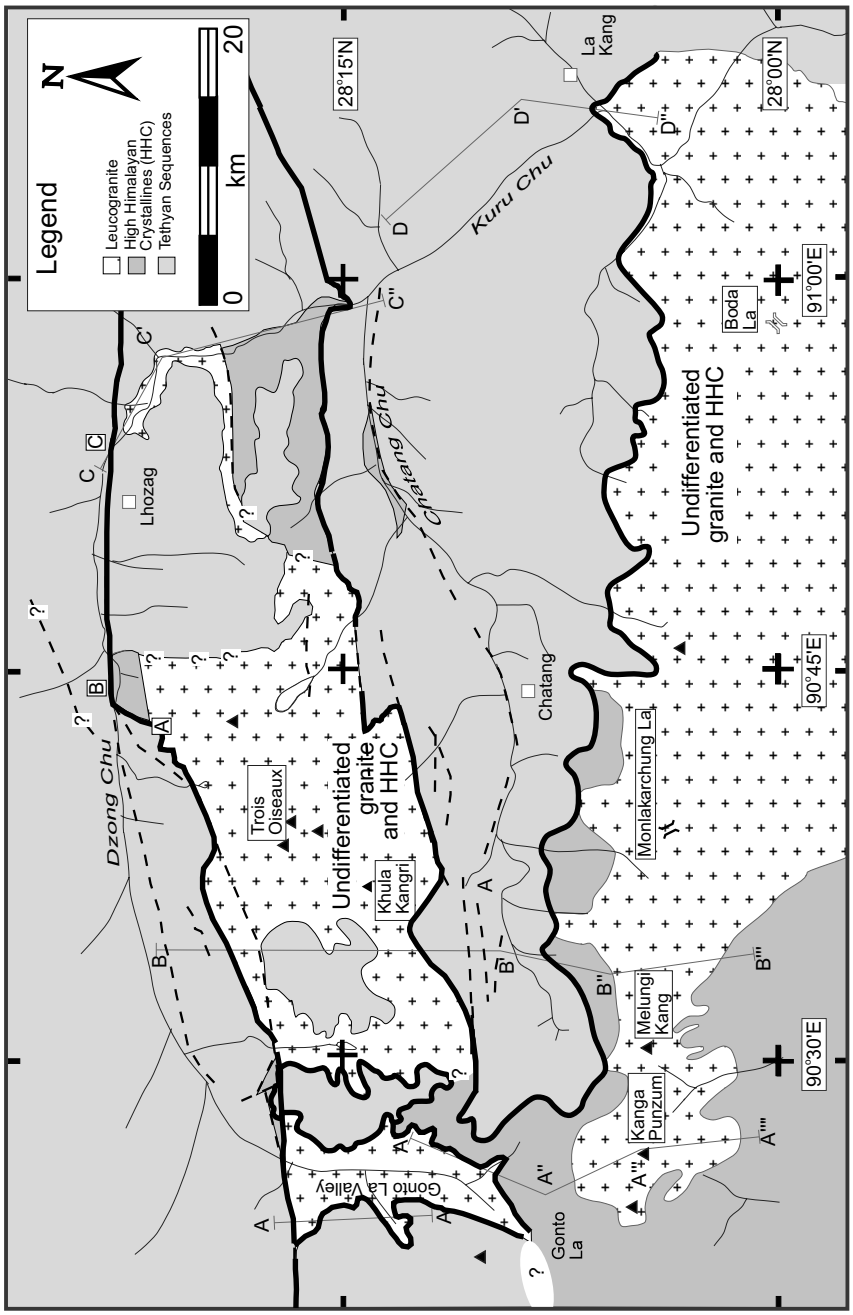

Figure 4.3 Summary of archival geologic map of Khula Kangri and Kanga Punzum-Monlakarchung massifs (see appendix A). Plus pattern: leucogranite; light grey fill: Tethyan (Mesozoic) sedimentary rocks; dark grey fill: High Himalayan crystalline rock (HHC); A-A' etc., are cross section locations. Letters in square boxes are locations referred to in text. Thick black line marks STDS. Dashed black lines are other faults. Question marks indicate specific uncertainty. For map sources, see appendix A.

Figure 4.4

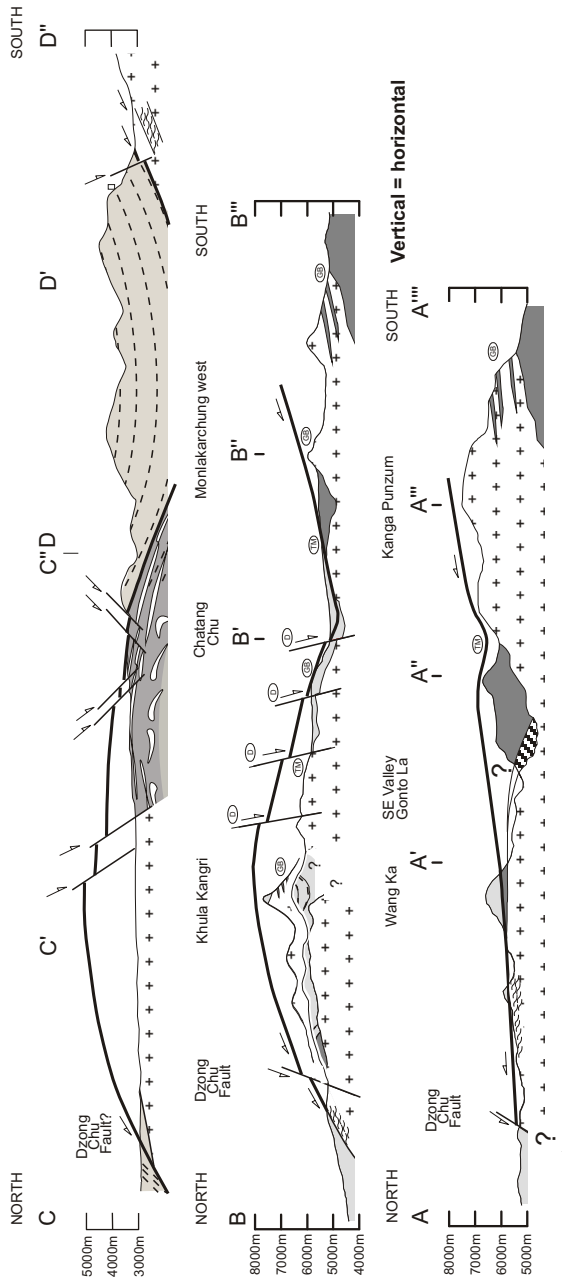

Figure 4.4 A, B, and C. Geologic cross sections continuous across both massif areas. Interpreted geology is either from Gansser (1983) in Bhutan ("GB") or interpolation from Thematic Mapper image ("TM"); see appendix A. Faults marked with "D" are approximate locations based upon topographic data. DCF is Dzong Chu Fault. A: cross section A-A"" is from DCF, through Gonto La valley to south of Kanga Punzum (A-A" is after Edwards et al., 1996). B: cross section B-B' is from DCF, across 7554 m summit of Khula Kangri to SW of Molakarchung La. C: cross section C-C'-D-D' is from Lozhag to La Kang, after Burchfiel et al. (1992).

Figure 4.5

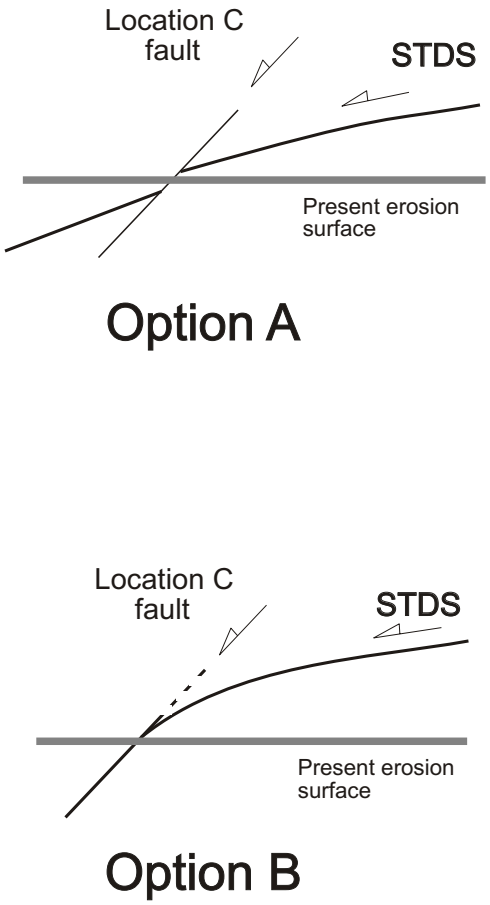

Figure 4.5 Cartoon illustrating the two options for the interpretation of the fault at location C, near Lhozag. In option A, the DCF is the fault, and cuts the detachment, displacing it , and slightly modifying the Gonto La detachment footwall / hanging wall contrast. In option B, the location C fault is the actual detachment.

Figure 5.1A

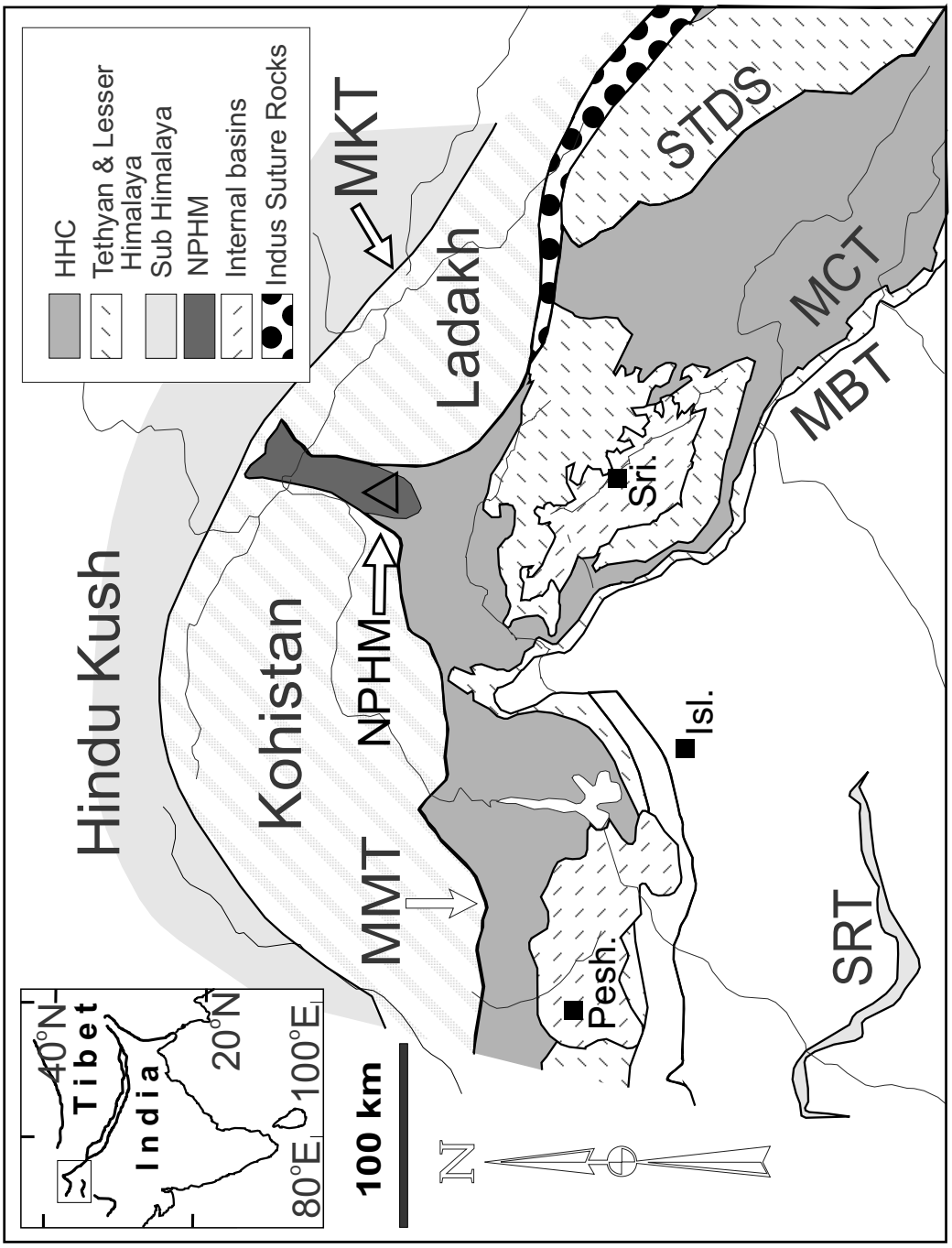

Figure 5.1A Regional Map of northwest Himalaya. MKT - Main Karakoram Thrust; MMT - Main Mantle Thrust; SRT - Salt Range Thrust, STDS - Southern Tibet Detachment System (section shown is Zanskar Shear Zone); MCT - Main Central Thrust; MBT - Main Boundary Thrust. Compiled by W.S.F. Kidd from Gansser, 1964; Coward et al., 1988; Searle et al., 1988; Greco and Spencer, 1993.

Figure 5.1B

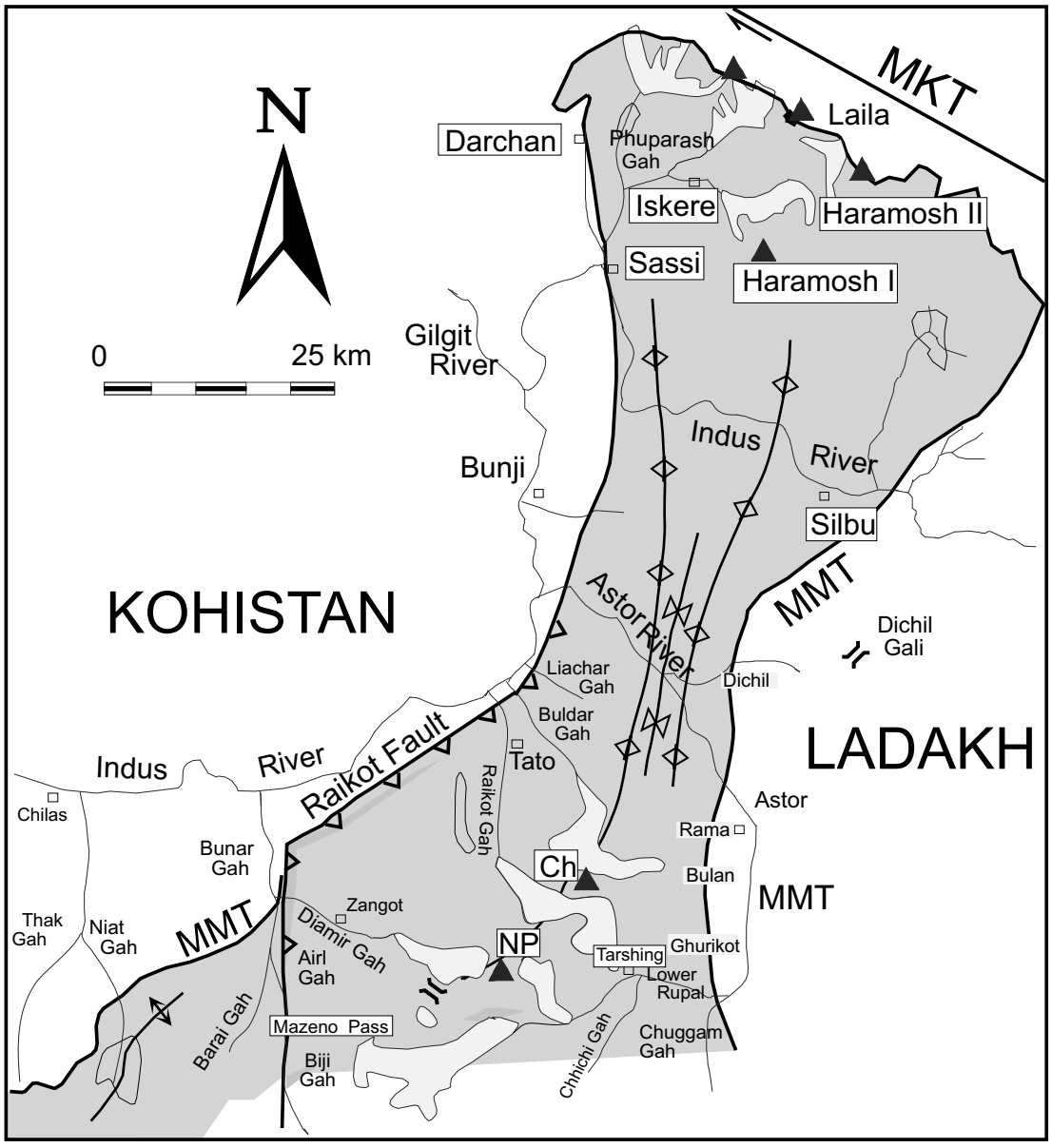

Figure 5.1B Overview map of NPHM. Selected valleys and towns shown. Grey - undifferentiated Indian rocks; white - undifferentiated KLS rocks or (north of MKT) undifferentiated Karakoram Terrane . NP - Nanga Parbat; Ch - Chongra Northern Peak; MKT - Main Karakoram Thrust. Heavy lines with barbs - reverse faults; paired barbs represent (W-E) Burdish Ridge Antiform, Dashkin synform, and Dichil Antiform, respectively (c.f., fig. 3). Black triangles - major peaks. Open squares - villages. Map sources: this study and Madin, 1986; Madin et al., 1989; Treloar et al., 1991; Lemmenicier et al., 1996; Pêcher et Le Fort, 1998.

Figure 5.2

Figure 5.2 A & B (next page)

A: (upper figure - next page) shows N-S cross sectional view of initial situation after S-directed thrusting along the MMT. A thick ductile, thrust sense, high strain horizon has developed (asymmetric fold symbols are general representation of sense of shear indicators found).

B: (lower figure - next page) shows equivalent W-E cross sectional view of A. Note use of "head and tail of arrow" (this convention is used throughout this thesis) indicating that the hanging wall ("Kohistan-Ladakh Series") has moved outward (with respect to the plane of view) while the footwall ("Indian rocks") has moved inward.

Figure 5.2

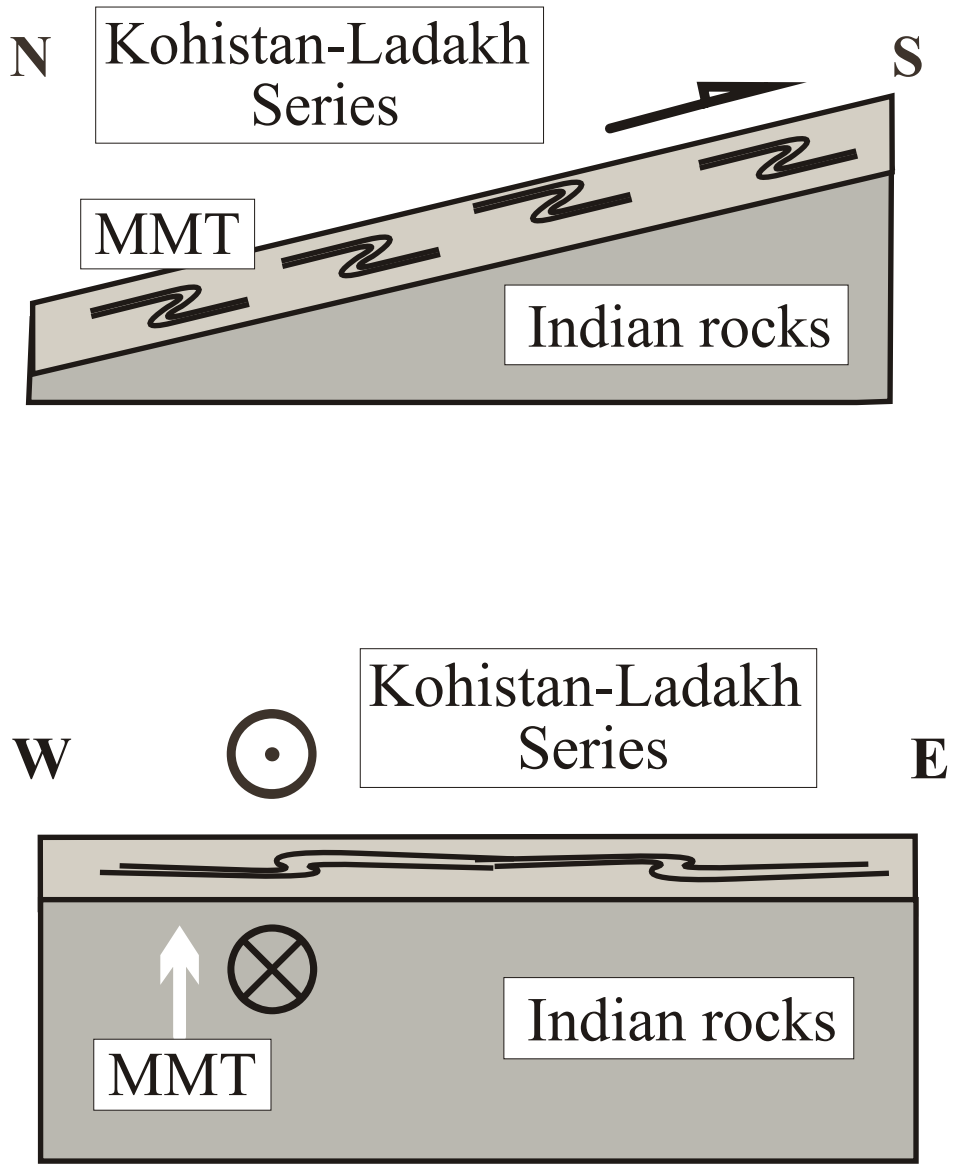

Figure 5.2A & B see previous page for caption

Figure 5.2C

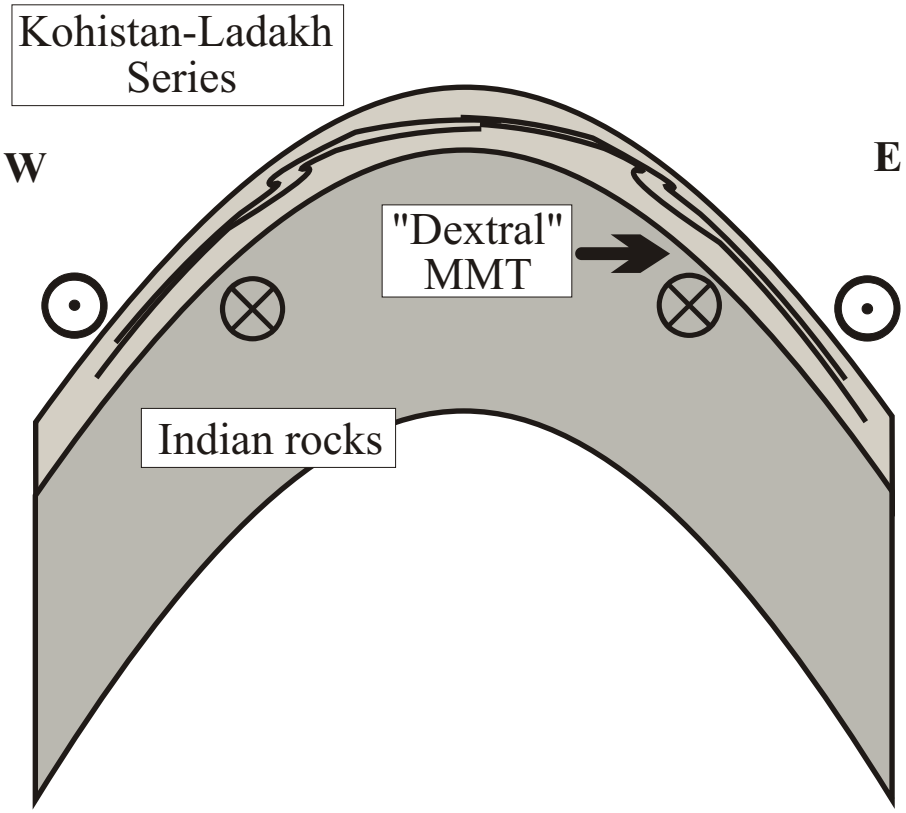

Figure 5.2C W-E cross sectional view of MMT after crustal scale antiformal folding. With continued tightening of the fold, steepening of limbs will bring the MMT high strain zone developed in 5.2A to near vertical. Apparent sense of shear will be left lateral on left (west) side, right lateral on right (east).

Figure 5.3

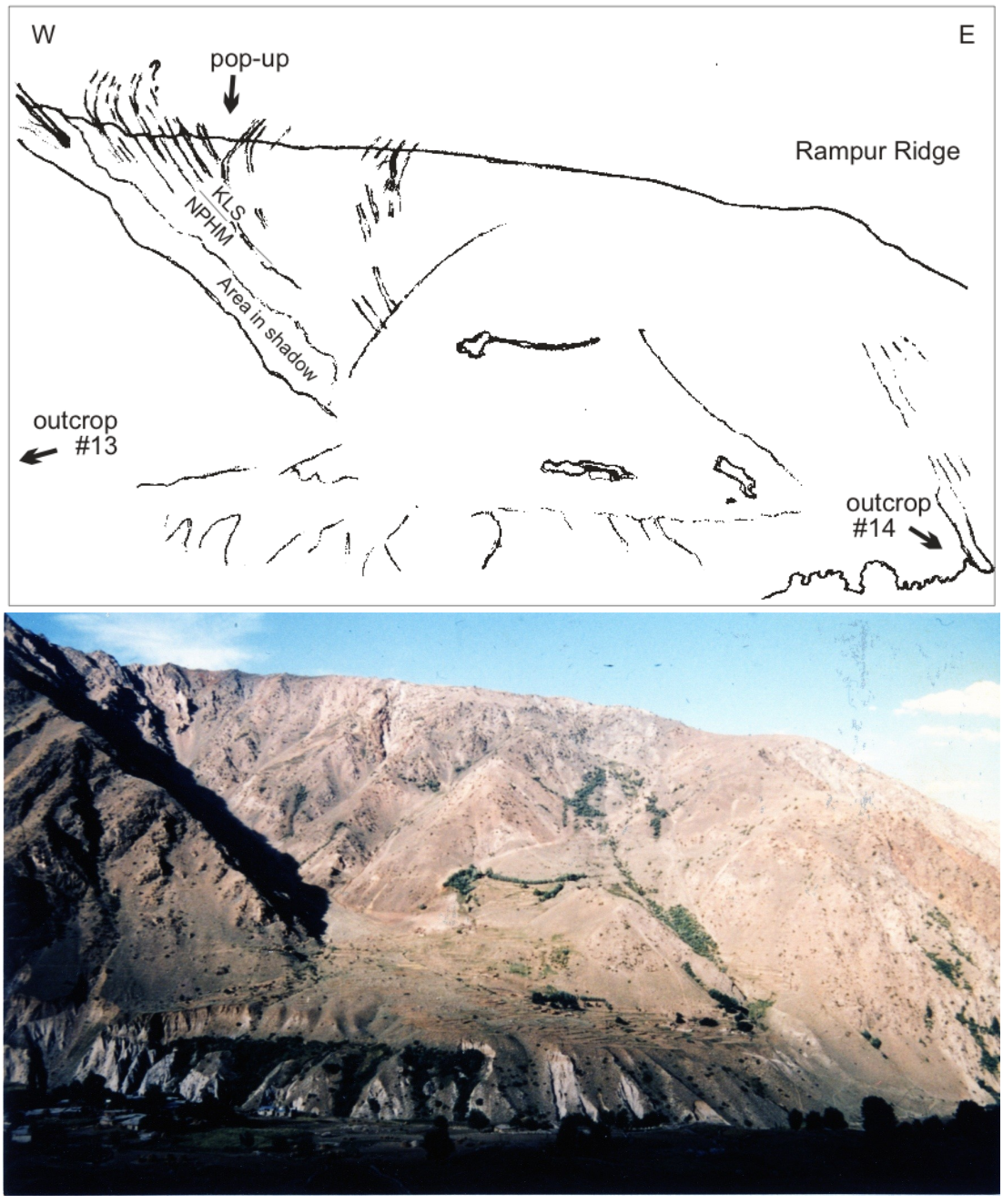

Figure 5.3 (field photo and line drawing). View to north of Rampur Ridge that forms easternmost portion of left bank of Lower Rupal Valley. Scattered fields and trees on level in foreground are ~2600 m in elevation. Central portion of Rampur Ridge is ~3700 m. Outcrop #14 is visible. Outcrop #13 is ~200 m beyond left edge of field of view. Contact between Kohistan Ladakh Series (KLS) and NPHM is present in hillside below Rampur Ridge and identified by pale brown east-dipping layers (labelled NPHM on line drawing) structurally below dark green layers (labelled KLS on line drawing). Note (1) local ~100 m wide pop-up structure and overturning of KLS layers east of pop-up. Photo 21/9/96 no.5.

Figure 5.4

Figure 5.4 Looking N. to left bank of Lower Rupal Valley. Cascade folding of mm-cm-10's cm layered garnetiferous metapelites interlayered with cm to 10's cm amphibolite and biotite schist. Trend is ~005° to 025° and axial planes dip ~65-75° W. Note overall monoclinal flexure is steep to left (west). Layers further steepen to left of field of view, and are overturned and truncated by a series of 40-80° west-dipping, brittle fault sets of west-side up minor (centimetre to metre) displacement. Jeep track is cut into hillside directly below field of view. Thickest dark band in lower centre is ~0.75m. Photo 21/9/96, no.3. View from right bank of Lower Rupal Valley.

Figure 5.5

Figure 5.5 Compositional layering within garnetiferous metapelites at outcrop #13, left bank of Lower Rupal Valley (c.f. fig 5.4). Note well-laminated quartzofeldspathic portions possibly suggesting high strain (c.f. fig. 5.8). Hammer for scale. Photo 6/7/95, no.5a

Figure 5.6

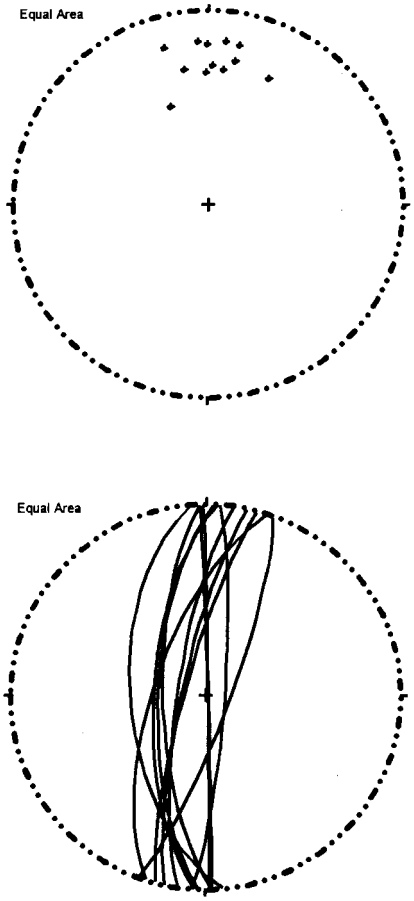

Figure 5.6 Lower hemisphere equal area projection of foliation poles and lineation of main fabric of all rocks in Lower Rupal Valley east of Tarshing.

Figure 5.7

Figure 5.7 Looking S and upwards, on right bank of Lower Rupal Valley (few 10's m W of outcrop #50). Mitch Wemple standing on cascade folds within layered garnetiferous metapelites. Trend is ~178° - 015° and axial planes dip ~68° W. Hinge lines plunge ~38°@005°. Note (1) prominent fold hinges in centre, and (2) crenulation intersection lineation developed below Mitch's left foot. Photo 21/9/96, no.4.

Figure 5.8

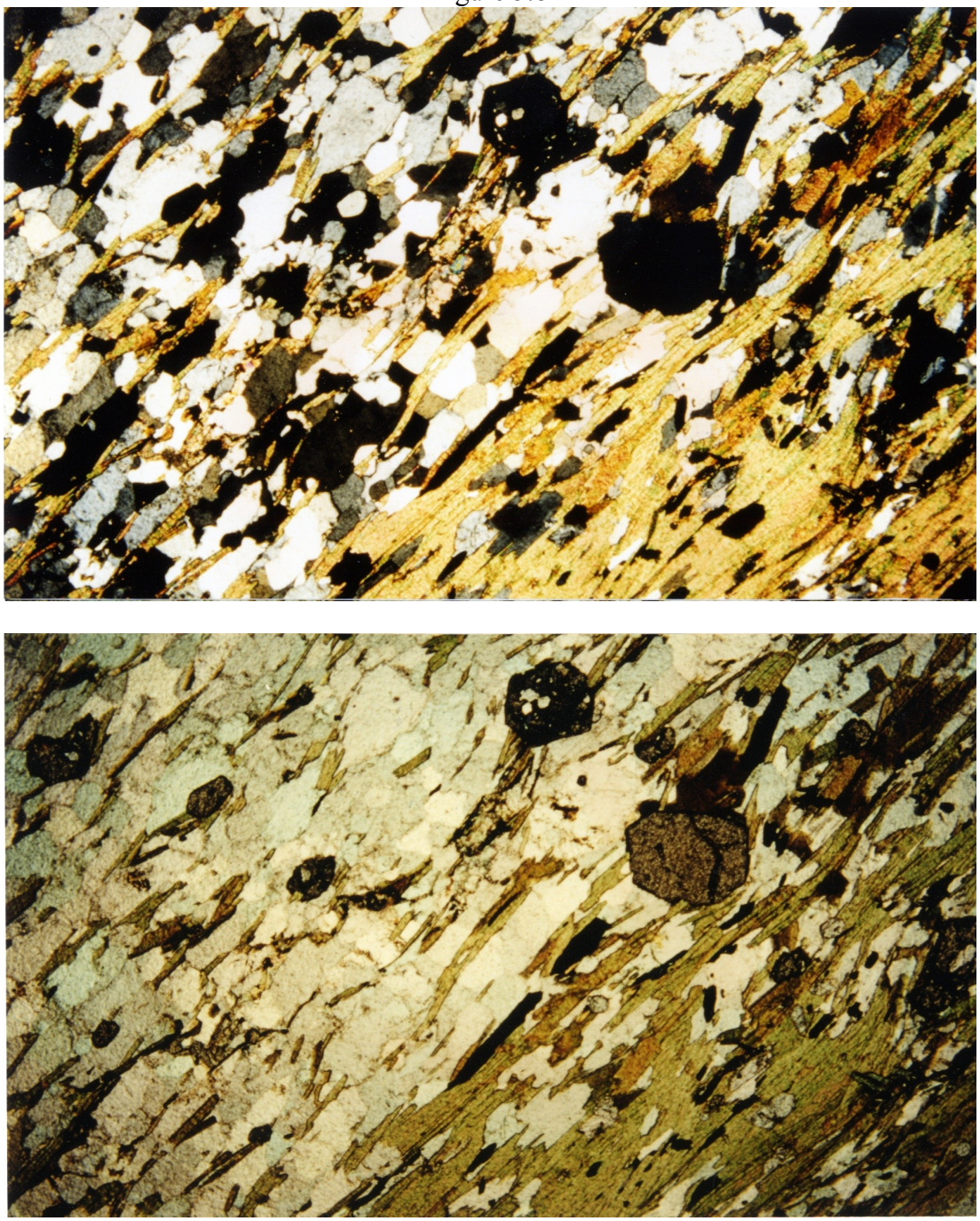

Figure 5.8 Optical photomicrographs (upper - crossed polars, lower - plane polarised light) of thin section 5/29F (cut from NE95/29-VI), garnet-biotite-amphibole schist from outcrop #13. Photo is taken with foliation oblique to horizontal to emphasise (1) proto-sedimentary layering (hornblende rich & poor portions) and (2) lattice preferred orientation in hornblende. See text for sense of shear discussion. South is to bottom left, north is to top right. Cut parallel with lineation (20°@005°), perpendicular to foliation (010°/85°E). Image base is 5.5 mm.

Figure 5.9

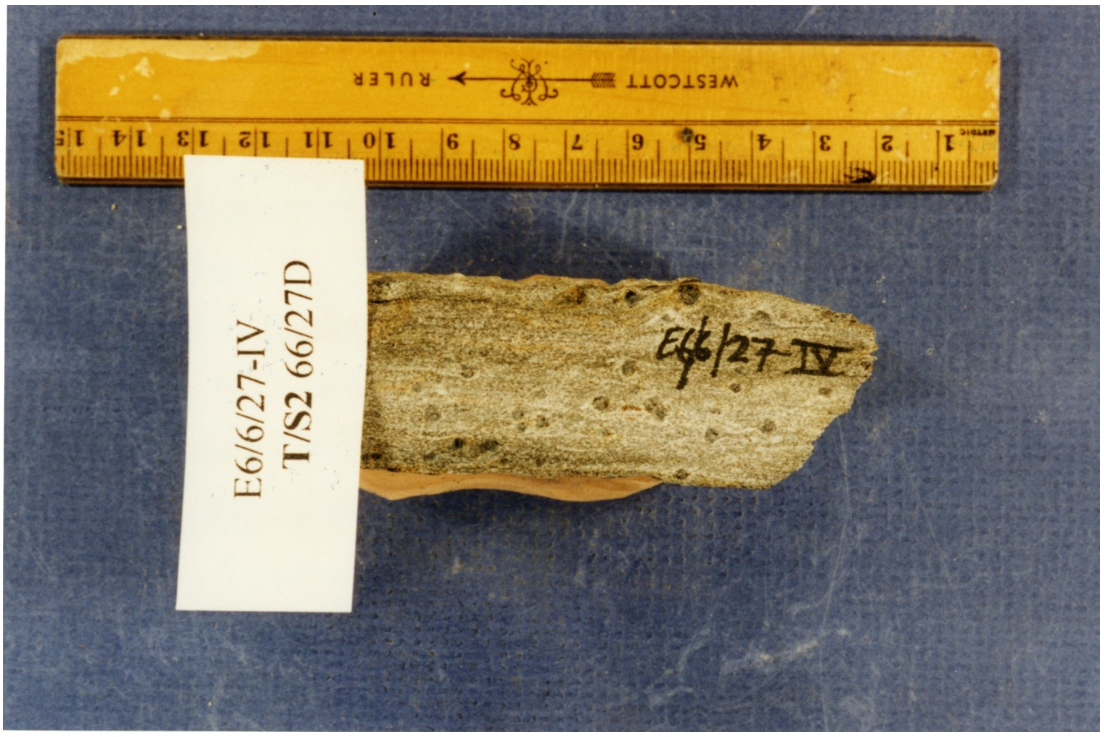

Figure 5.9 Sample E6/6/27-IV from near KLS/NPHM contact on left bank of E Astor Gorge. 170°/89°E, 15°@170°. Illustrates pressure shadow asymmetry in a garnetiferous metapelite. Sense of shear is dextral, consistent with fig. 5.10 (thin section 66/27D). This is typical for sense of shear observed in metasedimentary rocks along E. Astor Gorge.

Figure 5.10

Figure 5.10 (next page) Optical photomicrographs (upper - crossed polars. lower - plane polarised light) of thin section 66/27D, (cut from sample E6/6/27-IV). Illustrates pressure shadow asymmetry in a garnetiferous metapelite. Garnet shows good inclusion trails that suggest a rotation (in this case, clockwise i.e., dextral sense) of the garnet relative to the principal fabric defined by the micas (photomicrograph oriented with base of image approximately parallel to principal fabric). On all sides, the micas seem to bend around the garnet and there appears to be no post-kinematic growth. Other garnet porphyroblasts in this thin section are consistent. Sense of shear is dextral , consistent with other metasedimentary rocks along this part of E. Astor Gorge. Cut parallel with lineation (15°@170°), perpendicular to foliation (170°/89°E). South is on left. Base of image is 5.5 mm.

Figure 5.10

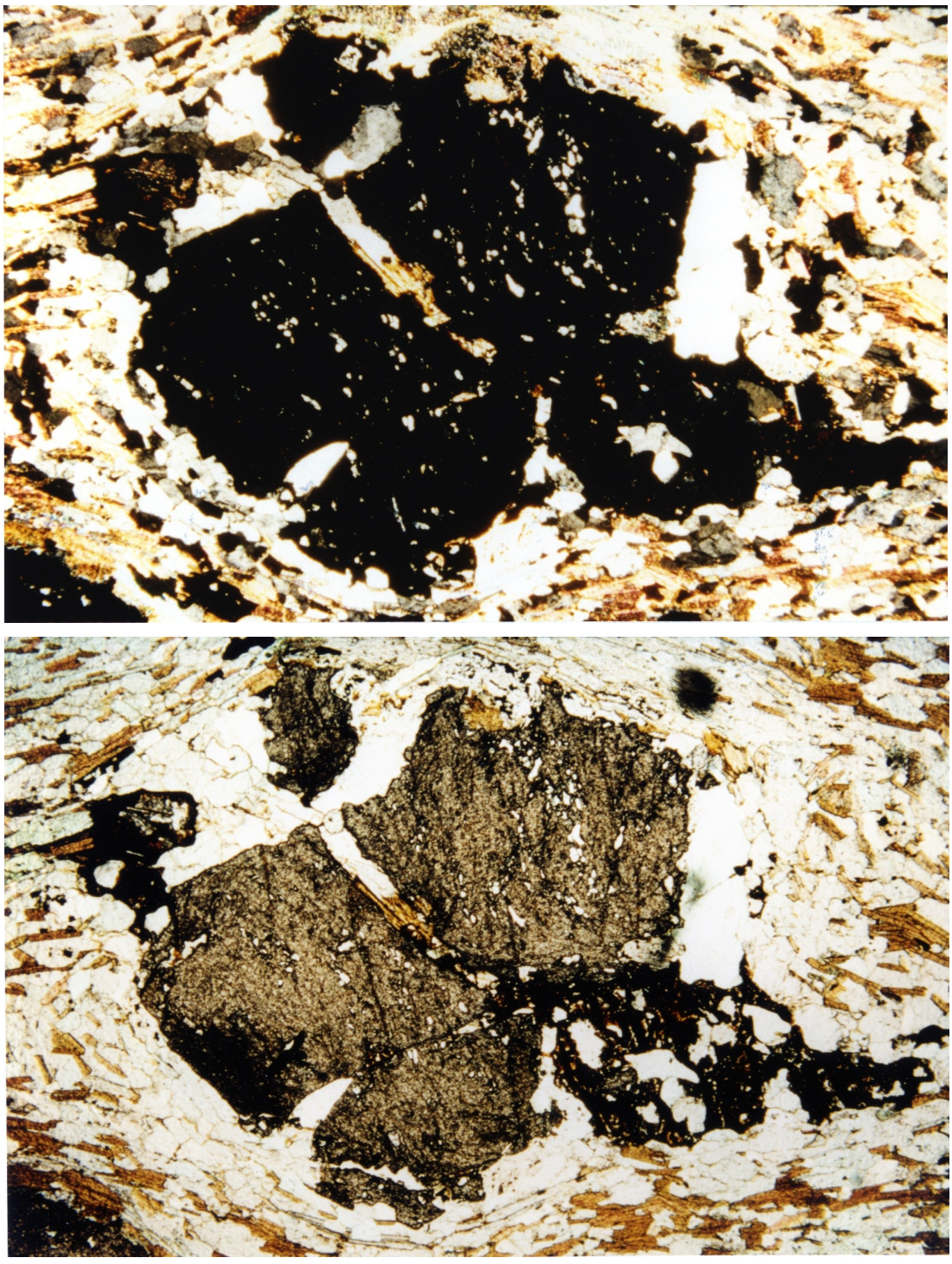

Figure 5.10 See previous page for figure caption.

Figure 5.11

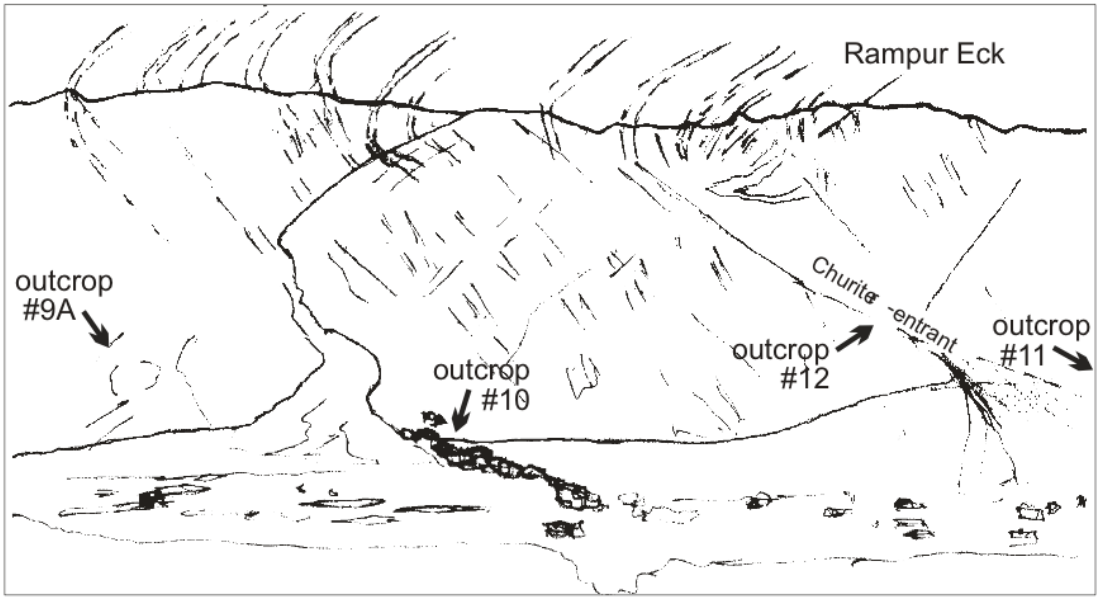

Figure 5.11 (field photo and line drawing). View to north of Churit Ridge that forms central portion of left bank of Lower Rupal Valley. Scattered low buildings and trees on level in foreground are Churit Village (2685m). Rampur Eck (west of Rampur Ridge) is 3884m. Outcrops #9A, #10, and #12 are visible. Churit re-entrant is marked byapparent closure of orange band and by fan descending to bottom right of field of view. Churit faults are distributed throughout re-entrant (see text). Travertine deposits of outcrop #10 coincide with freshwater spring and top of line of trees. Main layering above Churit is 70-89°E but appears less steep due to perspective. For discussion of steep/overturned layers, see text. Photo 21/9/96 no.8.

Figure 5.12

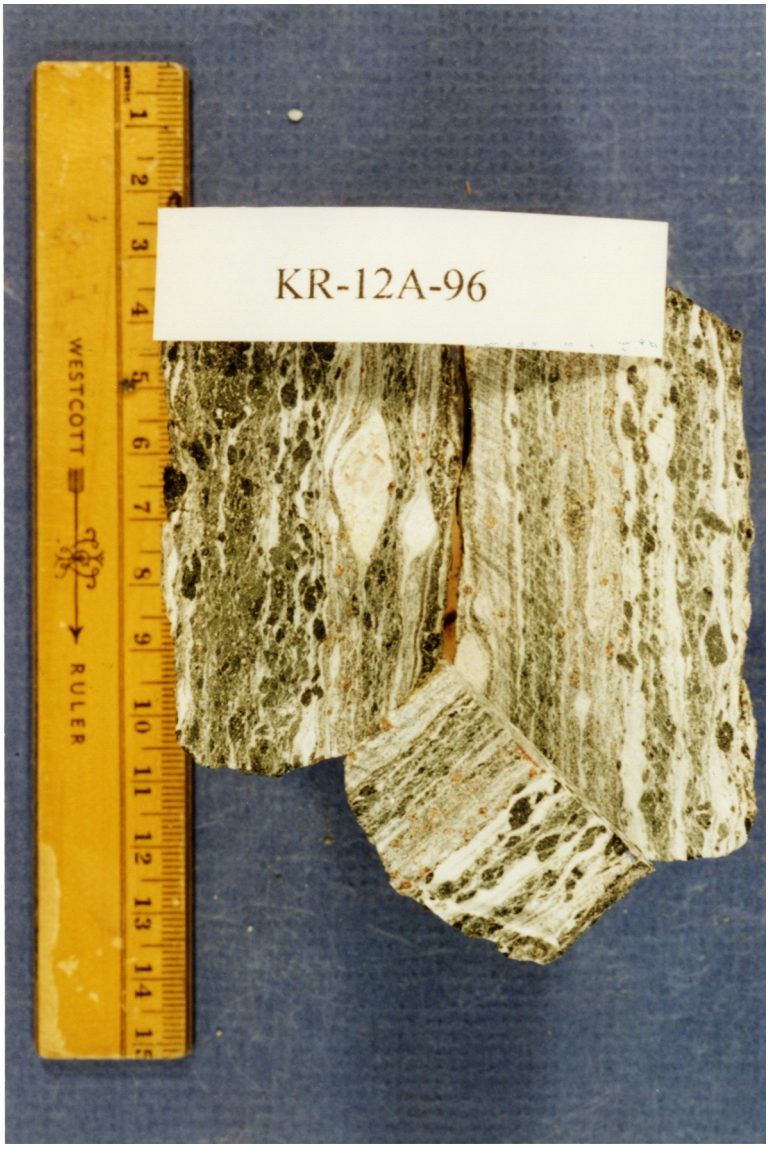

Figure 5.12 Photo of quartzofeldspathic-biotite-amphibolite gneiss found as float from scree on eastern edge of fan flowing out of Churit re-entrant. Very high strain is more clearly seen in fig. 5.13 (below).

Figure 5.13

Figure 5.13 High strain zone near outcrop #70A, within a ~60° west-dipping sequence of amphibolites, marbles and quartzofeldspathic gneiss on right bank of Bulan Gah. East is to left of picture, west is to right (note that layering of NPHM rocks throughout Bulan Gah dip gently to steeply west). Metre-scale boudins of amphibolite gneiss suggest sinistral sense of shear based upon boudin asymmetry and pinch and swell morphology. Also note asymmetric pinching fold adjacent to left hand side of flat top of main boulder in foreground suggesting sinistral sense of shear (flat top of boulder is approximately 3m wide). Photo 9/10/96 no.2, ~ 1.5 km upstream (W) from #70.

Figure 5.14

Figure 5.14 Angel hair unit at outcrop #62 on Rama left bank. Foliation: 159°/33°W, lineation: 7°@332°. Very stretched mm-scale rods of quartz and feldspar (where L>>S) define high strain zone. Note cm-scale compositional banding, mm-scale augen and rusty garnets. "Matrix" typically is greyish pink. Lens cap for scale. Photo 7/10/96 no.1.

Figure 5.15

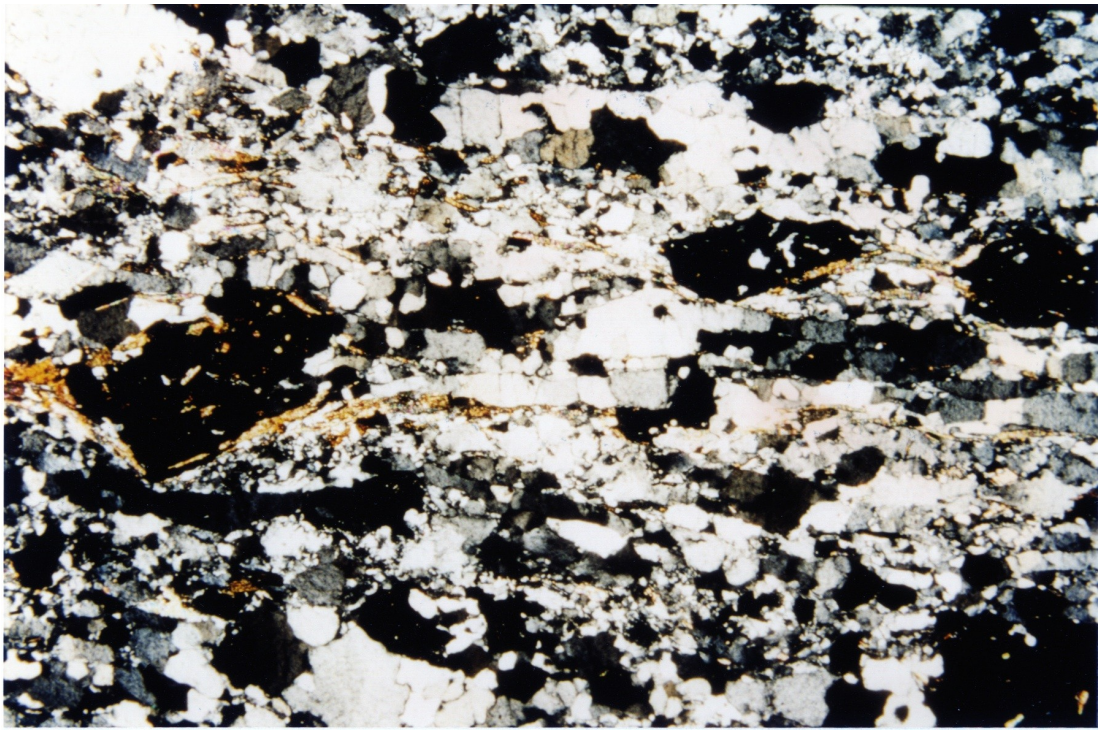

Figure 5.15 Optical photomicrograph of thin section 610/10A, (cut from sample E6/10/10-I, angel hair unit, ~750 m east of outcrop #73 on Dichil Gah left bank. 016°/53°W, 32°N-pitch). Illustrates likely tectonic grain size reduction based upon bimodal grain size distribution into ~300µm thick monomineralic quartz ribbons, and ribbons of very fine-grained (50-200µm) quartz and feldspar. Larger feldspar grains show suturing of margins to give partial core and mantle texture (not visible in figure). Sense of shear indicators are poorly developed both in figure and elsewhere in thin section. Left lateral is suggested by asymmetry of strain shadows and stepping of ribbons and trails associated with garnets, and slight development of oblique grains in lower part of picture. Cut parallel with lineation, perpendicular to foliation. South is on left. Base of image is 5.5 mm. Crossed polars.

Figure 5.16

Figure 5.16 Sample NE95/29-III, highly-strained garnet-biotite-quartzofeldspathic gneiss, immediately east of outcrop #12 (020°/40°W, 20° to N). Thin section (T/S2 5/29C - not shown) illustrates clear dextral shear sense based upon (1) oblique foliation of fine-grained component (~50-100µm), (2) tail asymmetry and strain shadows in quartz and feldspar augen (0.5-1.5 µm). (3) S-shapes in 100-300 µm quartz ribbons, locally bent & thinned at stress contacts ("corners") of clast margins, and (4) mica fish.

Figure 5.17

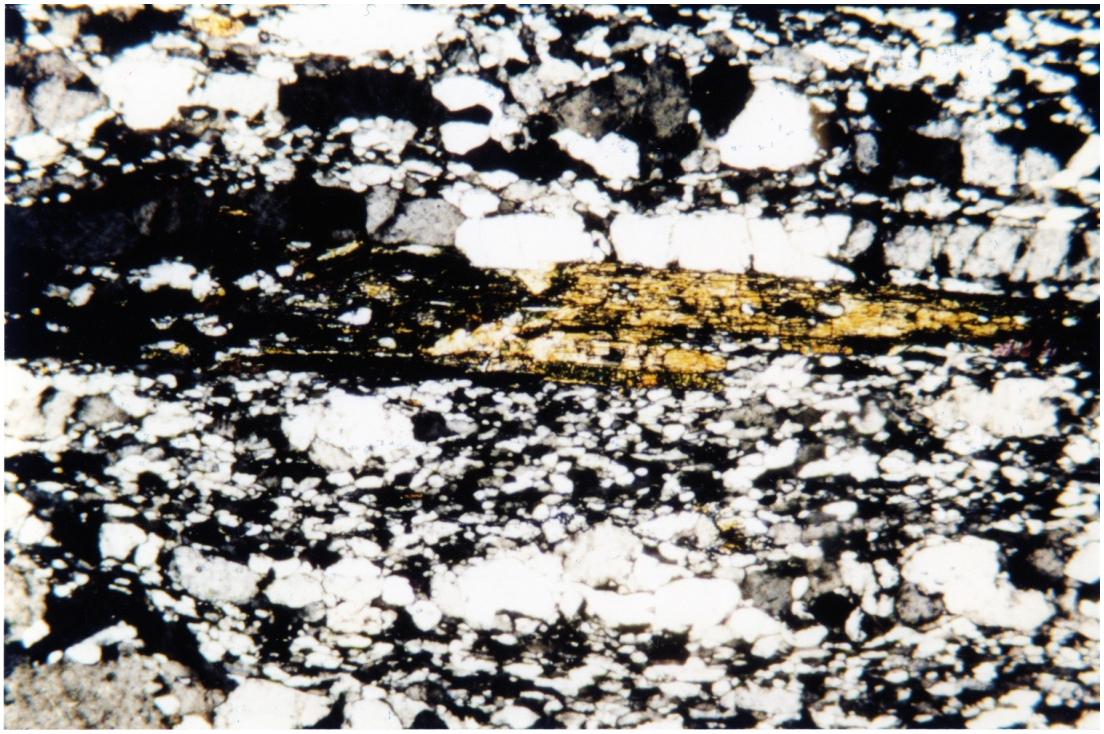

Figure 5.17 Optical photomicrograph of thin section 5/29D (cut from sample NE95/29-IV), fine-grained (50-100μm) L>>S granitic orthogneiss from west side of Churit re-entrant, ~50 m east of outcrop #12. Conditions of deformation are indicated by (1) C-surface parallel ribbons of quartz with even thickness (200-200 μm), (2) ~300 μm thick biotite grain that defines C-surface, (3) core and mantle appearance of certain feldspars (clearly seen in top left of photo) and (4) generally homogeneous flattening of <100 μm quartz groundmass (below biotite grain). Dextral sense of shear. Cut parallel with lineation (10°@359), perpendicular to foliation (180°/70°W). South is on left. Base of image is 5.5 mm and parallel with main fabric. Crossed polars.

Figure 5.18

Figure 5.18 Sample NE95/29-II, fine-grained L>>S garnet biotite quartzofeldspathic gneiss from outcrop #12 on west side of Churit re-entrant. Note blebs of quartz and feldspar stretched out into striking 1-3 mm thick rods indicating very high strain. Garnets (~2-5 mm) and quartz and feldspar augen show sigmoidal and deltoidal trails.

Figure 5.19

Figure 5.19 Optical photomicrograph of thin section 5/29B (cut from sample NE95/29-II), fine-grained (50-100µm) L>>S garnet biotite quartzofeldspathic gneiss from outcrop #12, west of Churit re-entrant. Prominent 0.25-0.75 mm monomineralic quartz ribbon suggests dextral sense of shear, as does oblique foliation (more conspicuous below ribbon). Dextral shear sense is also shown by mica fish, strain shadows on garnet and hornblende grains and tails from feldspar augen, elsewhere in thin section (not shown). Very finely sutured grain margins of large (1-3 mm) augen and fine (50-100 µm) groundmass indicate extensive grain boundary migration. Cut parallel with lineation (10°@005°), perpendicular to foliation (005°/89°W). South is on left. Base of image is 5.5 mm and parallel with main fabric. Crossed polars.

Figure 5.20

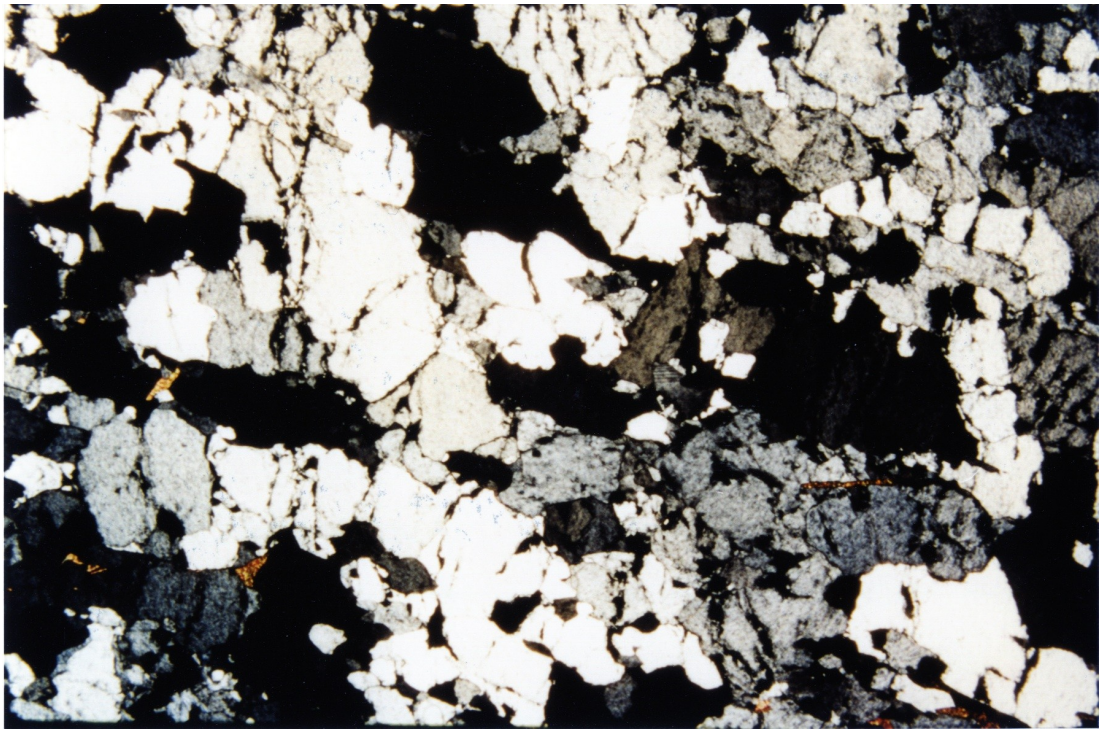

Figure 5.20 Optical photomicrograph of thin section 5/29A (cut from sample NE95/29-I, 020°/80°E; 20°N). Note generally "unstrained" appearance. Feldspars are clean; little to no significant patchy/undulose extinction. Some suturing of grain boundaries indicating limited operation of grain boundary migration. Note feldspars have "pitted" appearance. Large cracks in feldspars are not associated with extinction angle variation, suggesting lattice continuity. Cracks are inferred to be growth features (see text for discussion). Cut parallel with lineation, perpendicular to foliation. South is on left. Base of image is 5.5 mm and parallel with main fabric. Crossed polars.

Figure 5.21

Figure 5.21 Migmatite-rich portion of garnet-pelitic gneiss within general cover sequences (outcrop #69 - west of Churit Fault Zone in Ghurikot main valley). South is on left, view is from above. Foliation: 160°/65°W; lineation: 2°N. Based upon stepping directions of augen and leucosome tails, sense of shear is dextral, however, 1-2 cm long C'-surfaces (below arrow to top left of compass) trending NNE-SSW suggest sinistral sense of shear. Compass for scale. Photo 8/10/96, no.4.

Figure 5.22

Figure 5.22 Field photo looking north to left bank of main valley in Ghurikot Gah (near outcrop #68). Illustrates local buckling and fracturing associated with a zone of E-vergent displacement within Churit Fault zone. Note moderate west dip of overall gneissic layering and area in foreground where jointing is antiformally folded. Tree in top right of photo is about 8 m high. Photo 8/10/96, no.3.

Figure 5.23

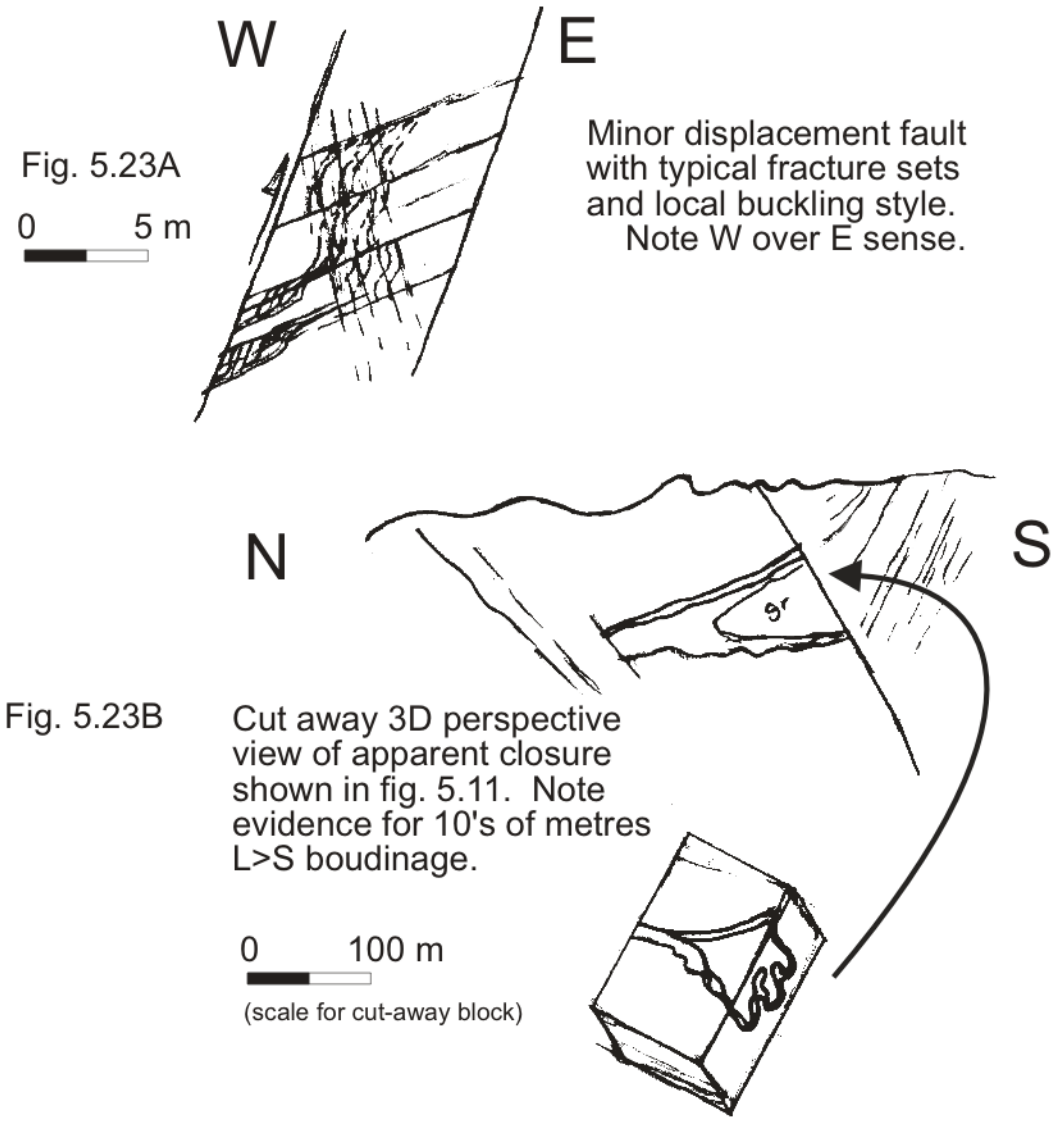

Figure 5.23 (A & B) Line drawings of field sketches around Churit re-entrant.
A. Illustrates typical E-vergent structure within Churit Fault zone. Layering is represented by monoclinally folded double lines. Low angle (~30°W) fracture planes are well-developed. Steeply, E-dipping fractures are less-developed.
B. Illustrates apparent closure is due to limited perspective of pinched out boudin (see text for discussion). Note ptygmatically folded base of boudin.

Figure 5.24

Figure 5.24 Field photo at outcrop #14 showing hornblende needles post-kinematically grown on foliation plane of very fine grained actinolite/tremolite schist (revealed by W.S.F. Kidd). Very continuous, even, m-cm compositional layering (not seen) suggests original metamorphism associated with high strain (see text for discussion). Rock is part of Kohistan Ladakh series (KLS). Photo 5/7/96, no.4.

Figure 5.25

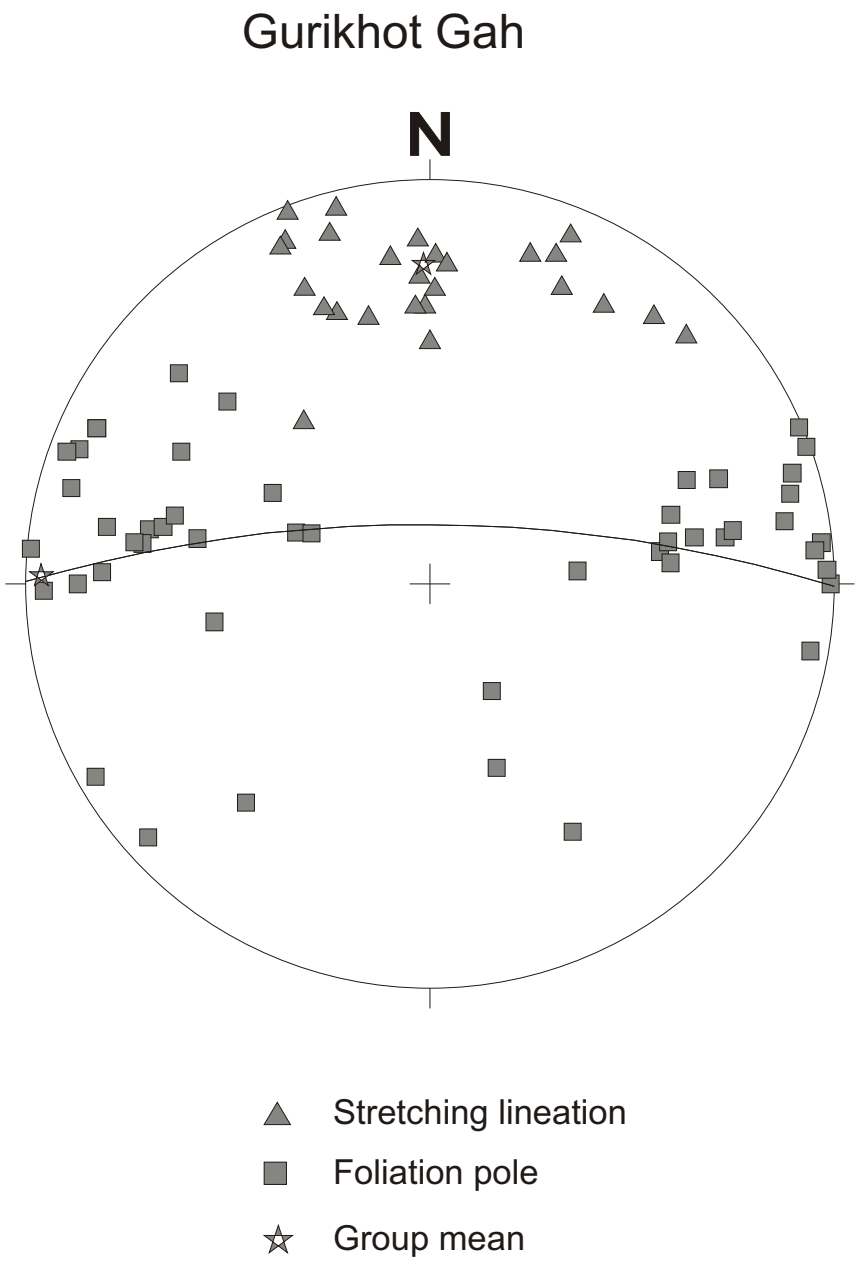

Figure 5.25 Lower hemisphere equal area projection of foliation poles and lineation of main NPHM rocks in three Ghurikot valleys.

Figure 5.26

Figure 5.26 Field photo looking north to left bank of main valley in Ghurikot Gah (near outcrop #66). Illustrates local folding associated with regional overturning of SE NPHM layering to W-dipping. Outcrop in bottom right is approximately 10 m high. Photo 8/10/96, no.1.

Figure 5.27

Figure 5.27 (field photo). View to west and upward to Bulan Peak (4915 m) showing ~500m (structural thickness) of NPHM metasedimentary rocks - schists and gneisses interlayered with marbles and amphibolites (recognisable as continuous black bands). Approximately 40°W true dip of foliation not clear due to perspective (see fig. 5.28). Photo 29/9/96 no.4. View from left bank of Astor Valley.

Figure 5.28

Figure 5.28 (field photo). Looking N. to left bank of Chuggam Gah, in Rattu area (3000-3500m main ridge in foreground). Small top of ridge just visible in centre of depth of field is Rampur Ridge (3884m). Bulan peak (4915m) clearly visible in distance. Crop fields are at ~2500m). In all visible portions of ridges, W-dipping (overturned) compositionally layered NPHM metasedimentary sequence is visible. c.f. fig. 5.28, Photo 24/9/96, no.2.

Figure 5.29

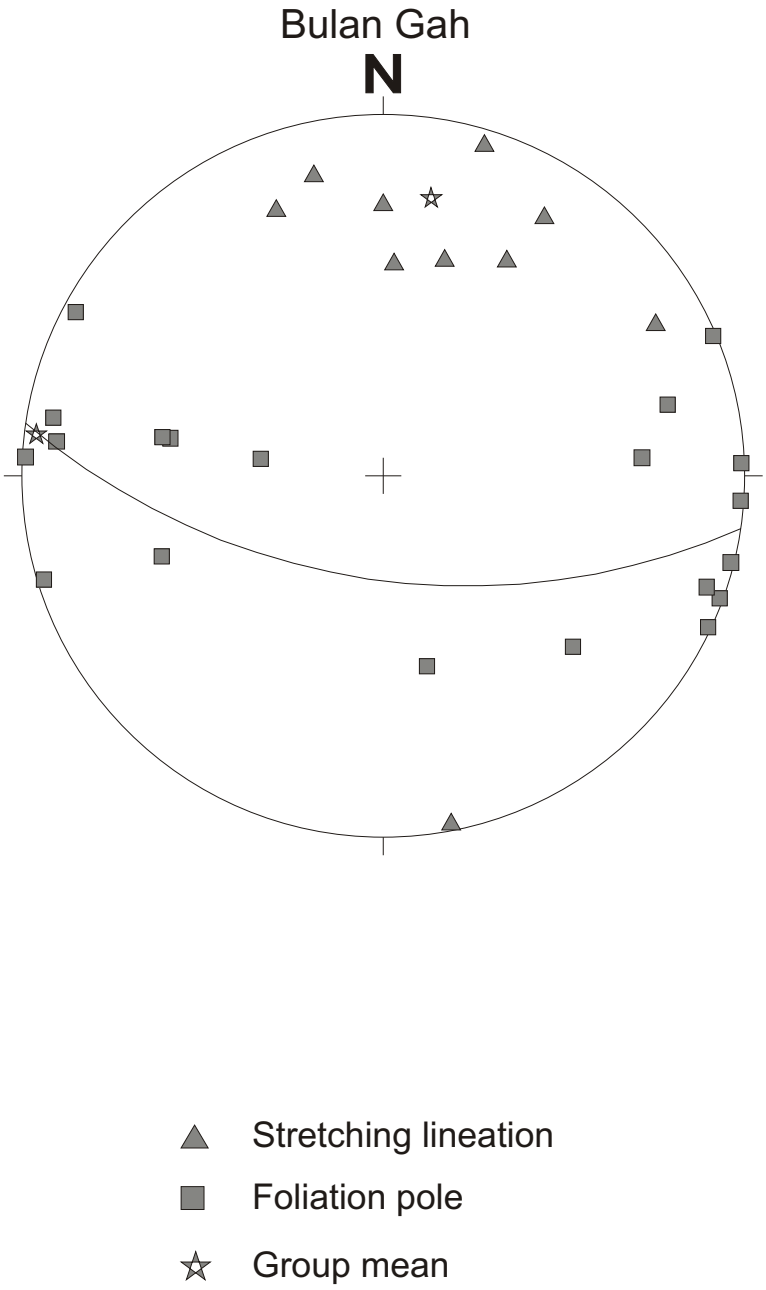

Figure 5.29 Lower hemisphere equal area projection of foliation poles and lineation of all rocks in Bulan Gah.

Figure 5.30

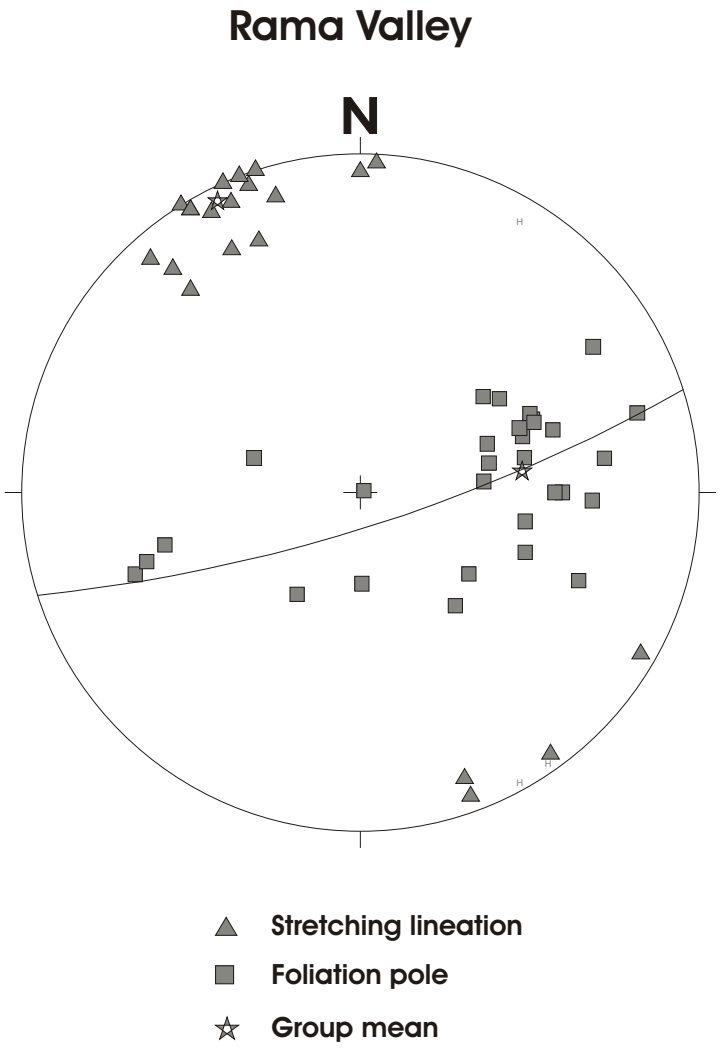

Figure 5.30 Lower hemisphere equal area projection of foliation poles and lineation of all rocks in Rama Valley.

Figure 5.31A

Figure 5.31A Lath unit outcropping on left bank of Rama Valley, ~300m east of outcrop #64. Note very disordered fabric picked out by generally non-preferred orientation of 1-4 cm laths of feldspar within biotite, garnet & quartzofeldspathic matrix. c.f. fig. 5.31B, taken ~10 metres nearby. Lens cap for scale. Photo 7/10/96 no.7.

Figure 5.31B

Figure 5.31B Lath unit outcropping on left bank of Rama Valley, ~300m east of outcrop #64. Indicates spectacular fabric gradient; portions with apparently greater shortening are visibly accompanied by change in foliation direction. Note foliation is highly variable and lineation only locally present. c.f. fig. 5.31A, taken ~10 metres nearby. Lens cap (55 mm) for scale. Photo 7/10/96 no.13.

Figure 5.32

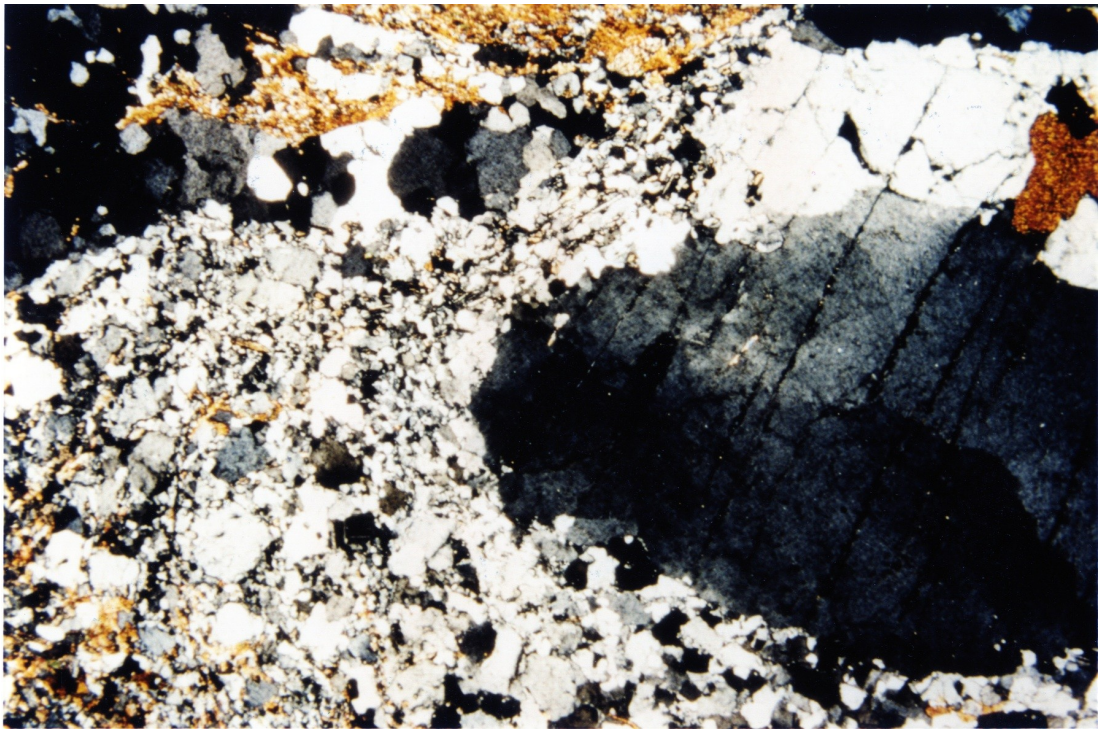

Figure 5.32 Optical photomicrograph of thin section AS/E, (cut from sample of same name, lath unit ~200m east of outcrop #71, on Astor Gorge left bank. 011°/43°W, 12°N-pitch). In upper left portion, 0.25-0.75 mm monomineralic quartz ribbon is typical appearance of quartz rich part of fine grained augen tail. Very finely sutured grain margins of large (>3 mm) feldspar clast and fine (50-150 μm) groundmass indicate extensive grain boundary migration recrystallisation. Not oriented. No sense of shear. Base of image is 5.5 mm long. Crossed polars.

Figure 5.33

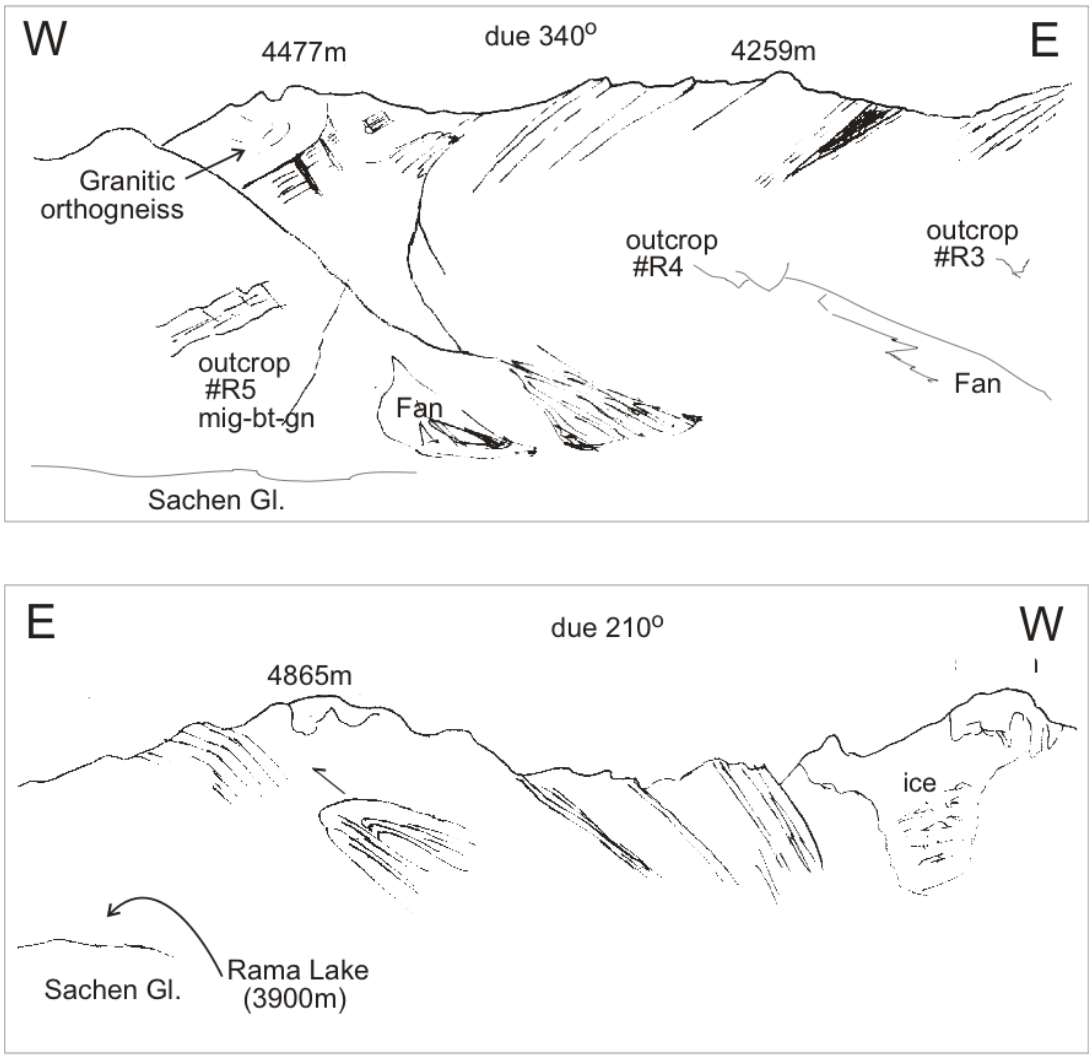

Figure 5.33 (line drawings of fieldbook sketches).
Upper: View to NW showing left bank of Rama Valley with 30-60°W dipping (overturned) compositionally layering of NPHM rocks. Between outcrops #R4 and #R5, gneisses pass into section of migmatisation. Note granitic orthogneiss in crags above outcrop #R5. Width of view is ~3 km.
Lower: View to SW showing right bank of Rama Valley with 30-60°W dipping layering of NPHM rocks. Fold and thrust in hillside clear but not observed close up in outcrop). Width of view is ~5 km. Sketches 6/7/97.

Figure 5.34

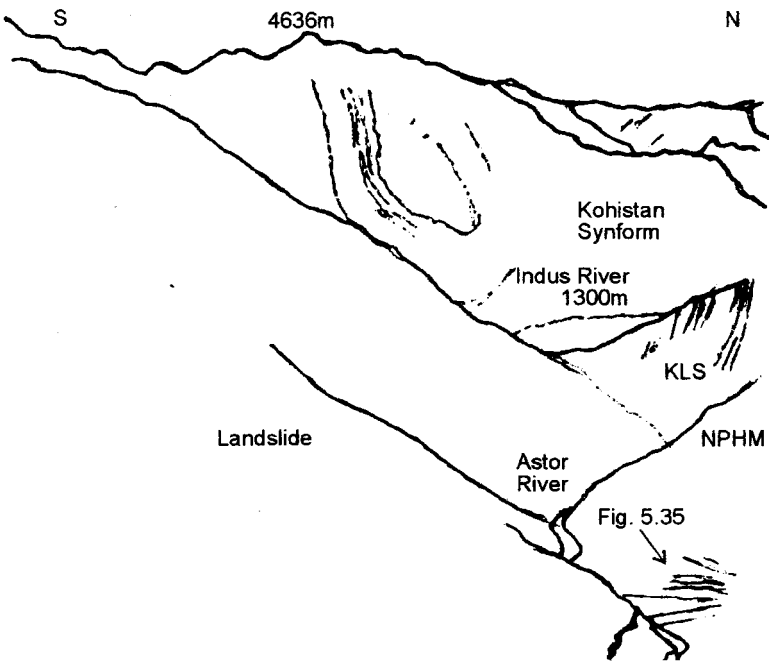

Figure 5.34 (field photo and line drawing). View to W over Indus River valley to Kohistan synform. Note contrast in NE dipping KLS layering and ~W dip of NPHM layering. Width of view ~2 km (foreground). Photo 6/7/96 no.0.

Figure 5.35

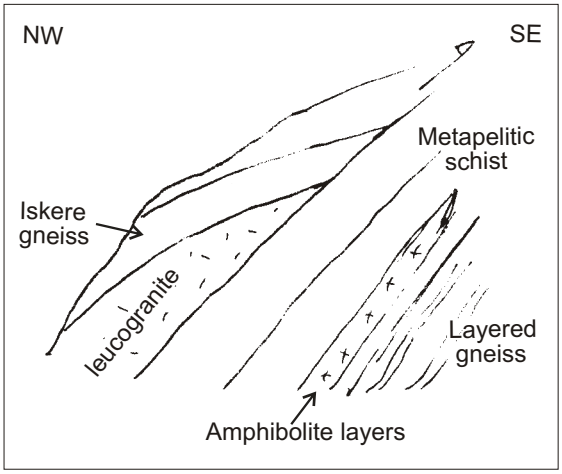

Figure 5.35 (line drawing of fieldbook sketch). View to NE and right bank of Astor Gorge, showing section of variable lithology near outcrop #A72. Note W-dipping layering is truncated by (1) E-vergent reverse faulting (fault propagation folds not shown), and (2) general E-W (ductile) extension. See text for further discussion. Width of view is ~0.5 km (c.f. location on fig. 5.34). Sketch composed: 26/6/96.

Figure 5.36

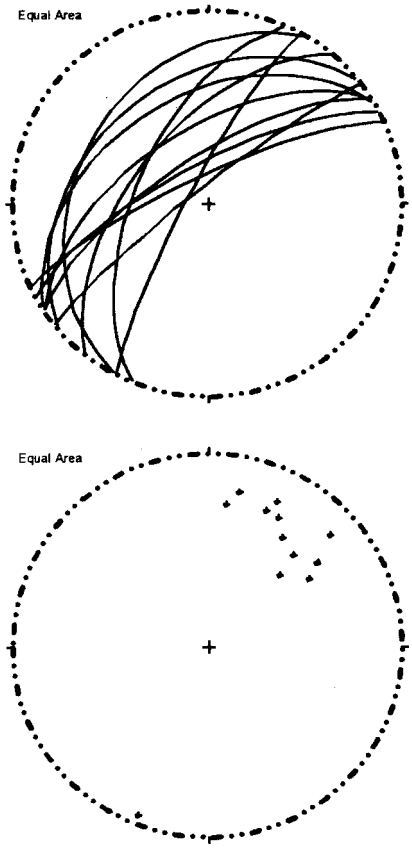

Figure 5.36 Lower hemisphere equal area projection of foliation poles and lineation of main NPHM fabric in W Astor Gorge.

Figure 5.37

Figure 5.37 Field photo of Iskere gneiss outcropping along left bank of Astor Gorge. Note characteristic finely foliated (023°/83°W, 22°@346°) grey granitic orthogneiss clearly cross-cut by migmatitic bodies (includes leucosome and melanosome). In photo, migmatitic bodies are isoclinally folded and sub-parallel to main foliation. Also common, however, are migmatitic bodies cross-cutting at high angles. Photo 10/10/96 no.10.

Figure 5.38

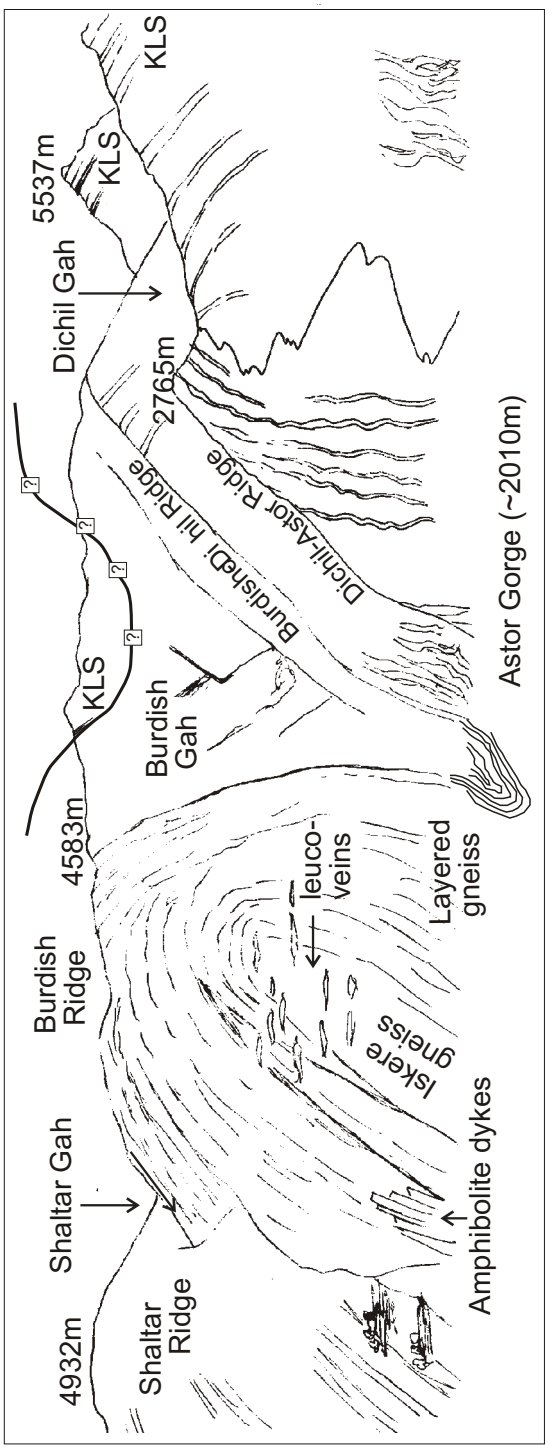

Figure 5.38 (line drawing of fieldbook sketch). View to NE from Astor Gorge high road looking to steep walls of right bank of Astor. Shows gneissic layering of Burdish Ridge antiform, Dashkin synform and some of Dichil antiform. See explanation in text. Width of view is ~10 km. Sketch composed: 7/7/97.

Figure 5.39

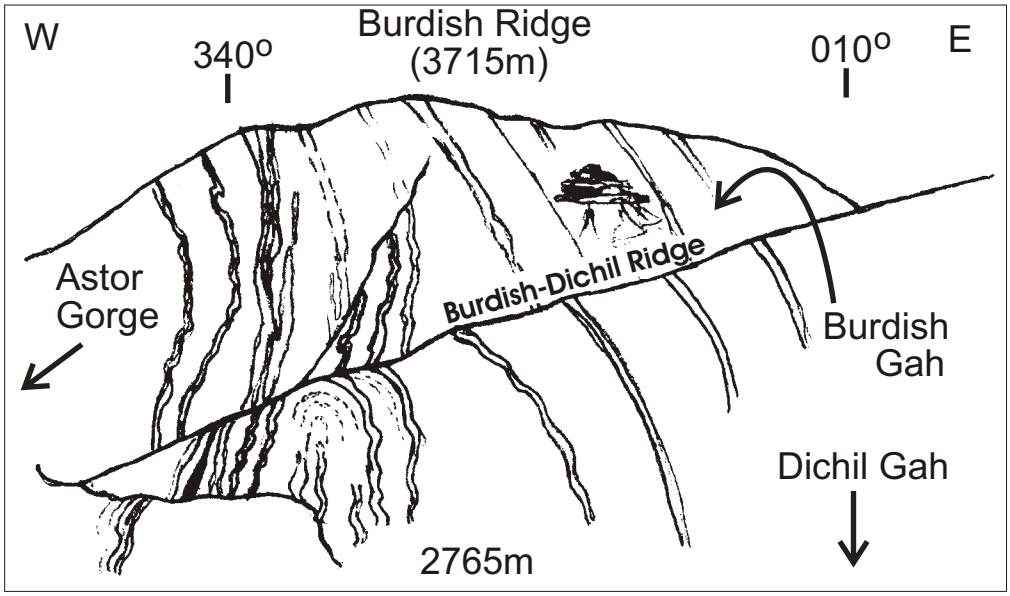

Figure 5.39 (line drawing of fieldbook sketch). View to NNW showing antiformal folding of gneissic layering clearly exposed upon wall of right bank of Lower Dichil Gah (Burdish-Dichil Ridge. View is from Dichil Pass (2765m). Antiformal closure is not seen in wall of Burdish Ridge because of ~NNE trend of axial trace of fold and viewer's NNW perspective from Dichil Pass. Antiformal closure intersects significantly to right of field of view. Apparent eastern limb of antiformal closure seen in wall of Burdish Ridge in left of sketch is eastern limb of Burdish antiform ("western antiform"). Dashkin synform is out of view down in Burdish Gah. Width of view ~3 km. Sketch composed: 10/10/96.

Figure 5.40A

Figure 5.40A Migmatite-garnet-pelitic gneiss at foot of Dichil Pass trail, ~200m below outcrop # 72 (Foliation: 007°/89°W, hinge intersection lineation 25°@007°). Note leucosome portion is isoclinally folded and lacks a strong melanosome. Swiss knife for scale. Photo 10/10/96 no.2.

Figure 5.40B

Figure 5.40B Cascade / parasitic folding within well-stretched amphibolite interlayered with migmatite-garnet-pelitic gneiss. Elsewhere (in large isoclinal hinge sections) amphibolite is seen to cross-cut migmatised gneissic foliation. Note crenulation intersection lineation clearly developed beside compass. Foot of Dichil Pass trail, ~200m below outcrop # 72 (hinge lineation 22°@011°). Compass for scale. Photo 10/10/96 no.6.

Figure 5.41

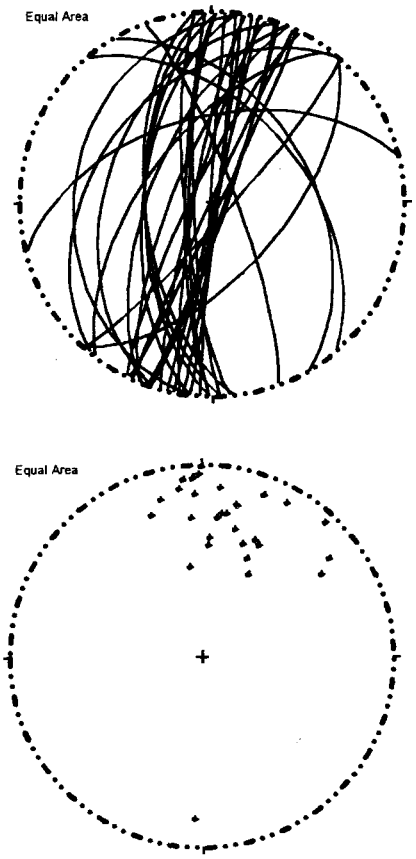

Figure 5.41 Lower hemisphere equal area projection of foliation poles and lineation of main NPHM fabric in eastern Astor Gorge and Dichil valleys.

Figure 5.42

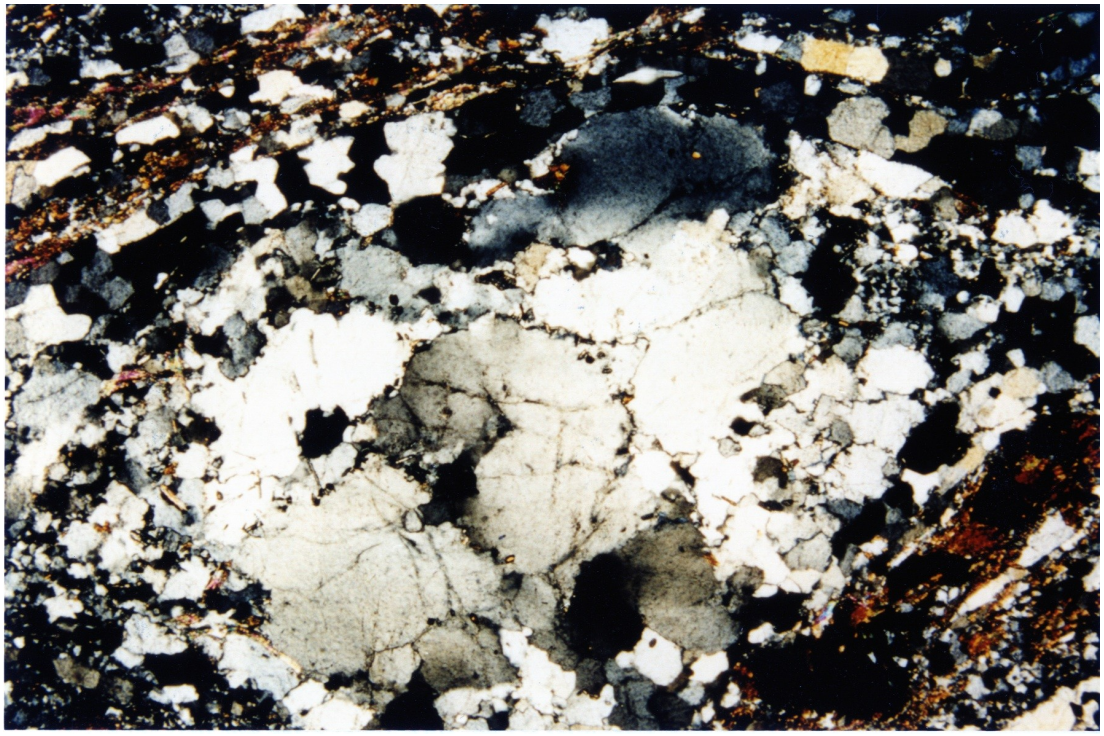

Figure 5.42 Optical photomicrograph of thin section 66/27E (cut from sample E6/6/27-V, not shown), deformed portion of lath unit on eastern Astor Gorge left bank, ~300m W of outcrop #71. Conditions of deformation are indicated by (1) C-surface parallel ribbons of quartz with even thickness (200-400 μm), (2) C-surface defined 100-200 μm thick biotite grain, (3) >3 mm feldspar clast with sutured internal grain boundaries indicating onset of grain boundary migration and beginnings of core and mantle texture within grain. Grain boundary migration and wholesale grain size reduction have operated extensively (both in field of view and elsewhere in thin section) as indicated by very fine (50-100μm) grain size of surrounding quartzofeldspathic component. C-S fabric elsewhere in thin section clearly shows dextral shear sense. Cut parallel with lineation (14°N), perpendicular to foliation (060°/38°E). South is to right. Base of image is 5.5 mm and parallel with main fabric. Crossed polars.

Figure 5.43

Figure 5.43 Granitic orthogneiss in Rupal side valley at outcrop #18. This type of granitic orthogneiss is ubiquitous to the Rupal-Chichi shear zone. Asymmetric fabric is marked by (1) biotite planes clearly forming S and C surfaces. and (2) thin 0.5-20 mm feldspar porphyroclasts with asymmetric tails. Foliation is 040°/80°W and stretching lineation plunges 50° towards 238°. Sense of displacement is NW side upwards and vergent towards NE (dextral shear).
Photo 7/10/96 no. 13..

Figure 5.44

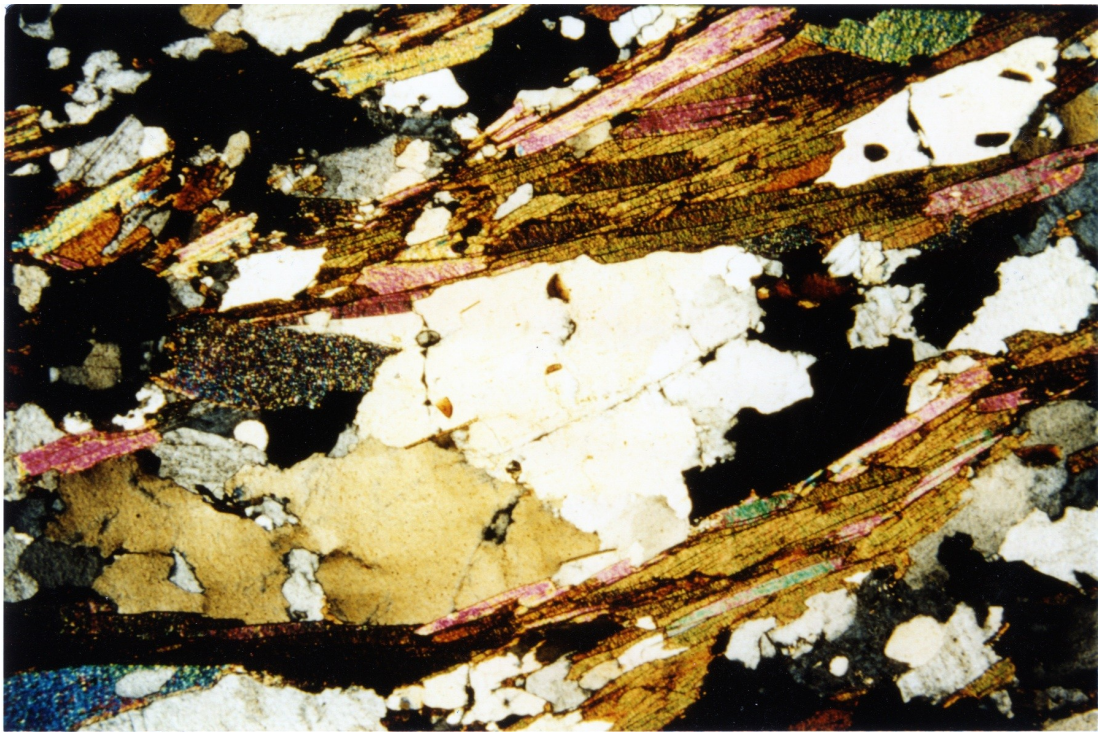

Figure 5.44 Optical photomicrograph of thin section 66/18D (cut from E6/6/18-IV, not shown), ~1 km NW of #18. Shows characteristic microstructure of RCSZ orthogneiss deformation conditions (note finer grained portion hence >2 mm feldspar porphyroclasts not shown). Sense of shear clearly dextral based upon sigmoidal feldspar porphyroclast tails; 600-1000 μm biotite surfaces define C and S surfaces (distinct in overall thin section). Note coarseness of grains and only very slight suturing of internal grain boundaries. Some recovery may have operated but lack of evidence for significant subgrain rotation recrystallisation within grain suggests less than 400°C temperature of deformation. Cut parallel with lineation (50°@238°), perpendicular to foliation (040°/80°W). South is to left. Base of image is 5.5 mm and parallel with main fabric. Crossed polars.

Figure 5.45

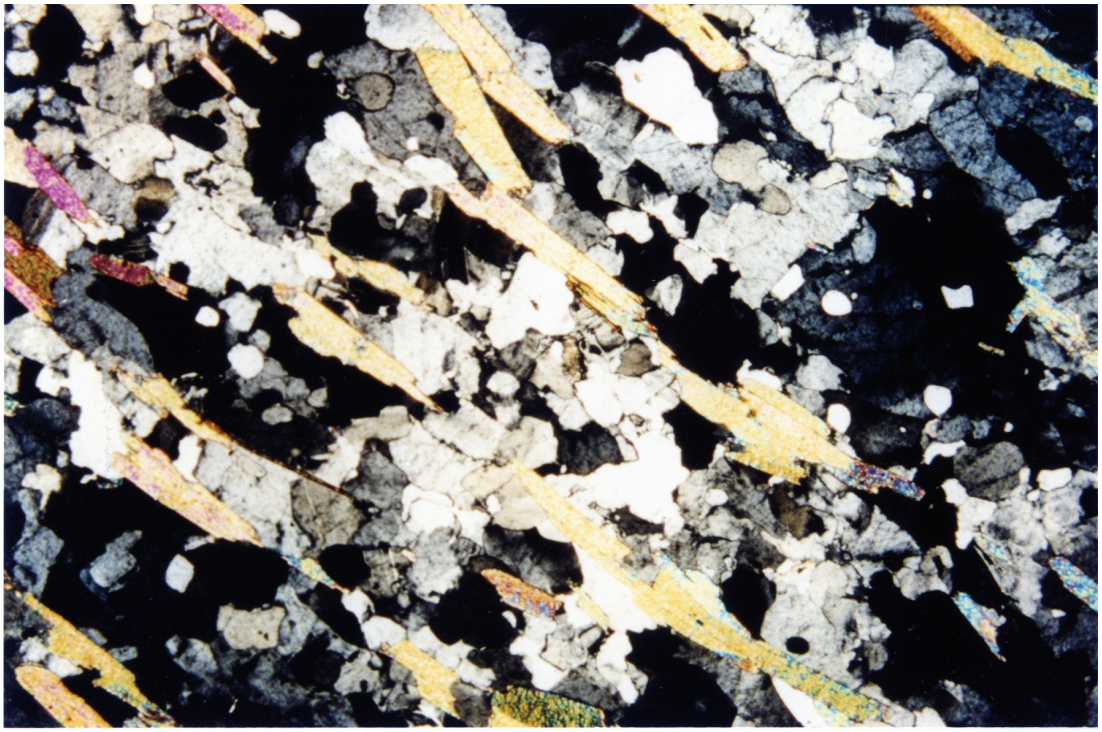

Figure 5.45 Optical photomicrograph of thin section cut from KC-9A, collected ~300 m north of outcrop #CC4, illustrates microstructure of granitic dyke cross-cutting main RCSZ granitic orthogneiss. Note lack of strain evidence in quartzofeldspathic portions; grains have even extinction and grain size distribution is small. Preferred lattice orientation of biotites is likely a product of super solidus strain. Sample from loose block not possible to orient. Base of image is 5.5 mm. Crossed polars.

Figure 5.46

Figure 5.46 View to NW of general area of #CC5 in southern Chichi Nallah. photo shows moderately WNW dipping sequence of metapelitic schists interlayered with quartzite, marble and amphibolite. Snow covered, tan-coloured hills in background at right of picture are granitic orthogneiss. Contact between granitic orthogneiss and metasedimentary sequences is immediately below snow covered top of ridge in foreground. This is ~500m from fan at base of picture. Metasedimentary sequences are fully concordant with the granitic orthogneiss (see text for discussion).

Figure 5.47

Figure 5.47 Photo showing tight folding in quartzite layers within metasedimentary sequences in general area of #CC5 (portion of outcrop shown in fig. 5.46). Hinge plunges 22° towards 223°, average local foliation: 023°/71°W.

Figure 5.48

Figure 5.48 Photo showing isoclinal asymmetric folding in quartzite layers separating biotite schist (right) from granitic orthogneiss (far left) in general area of #49a. Hinge plunges 62° towards 343°, average local foliation: 152°/58°E. Fold asymmetry indicates east limb of antiform, consistent with nearby observation.

Figure 5.49

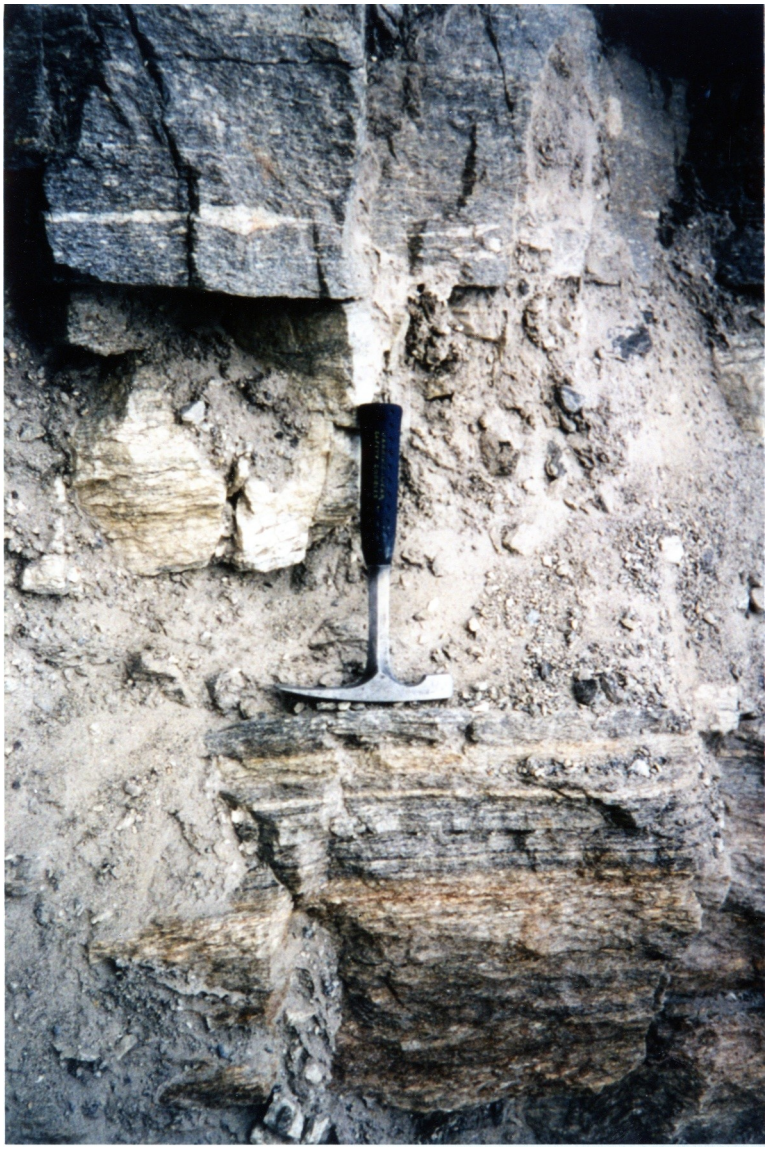

Figure 5.49 Photo in vicinity of outcrop #54 - Mazeno Low Camp, showing moderately north-dipping compositionally layered gneiss (locally including metasediments). Stretching lineation is 36°@317°.

Figure 5.50

Figure 5.50 Photo from #CR52 looking towards West Shagiri ridge, showing WSW trending metasedimentary and compositionally layered gneiss forming tight overturned steeply N-dipping synform, picked out by dark amphibolite layers. Fan in central portion is spilling down from Rupal left bank #1 Glacier. To left (west) of fan is granitic orthogneiss of #Sh2, to right are metasediments of #Sh1. Bottom of photo is ~3800m, ridge top in foreground is ~5500m. Note slight kinking in steeply N-dipping compositionally layered gneisses in background to far left of field of view.

Figure 5.51

Figure 5.51 (next page) Looking N to summit of Nanga Parbat (8143m), from #CR52 on Shaggin Glacier left bank. Nearly 5 km of relief is visible; long moraine ridge at foot of photo is Shagiri Glacier, and base of photo is ~3600m. Note ~50° NW dipping layer of black gneiss forming upper 400m of summit of Nanga Parbat. Below are thick sequences of granitic orthogneiss with local 100's metres thick leucogranite plutons. ~1.5 km thick pluton to left is characterised by "hooked boudin" xenolith. Extensive, cross-cutting pegmatitic dykes (part of 1.2 - 2.4 Ma suite) are just visible at bottom right. Lower regions of field of view contain ductile to brittle SE-vergent reverse faults, some of which show good evidence for later normal motion (see text for discussion).

Figure 5.51

Figure 5.51 (see previous page for caption).

Figure 5.52

Figure 5.52 Photo looking to NW to left bank of Toshain Glacier. Shows steeply W-dipping (and S-plunging lineation) fabric of compositionally layered gneisses interlayered with granitic orthogneiss in lower part of field of view decrease in dip sharply upwards. A thrust is inferred to separate lower rocks from moderately N-dipping compositionally layered gneisses interlayered with granitic orthogneiss above (see text for discussion).

Figure 5.53

Figure 5.53 Photo looking to NE to Nanga Parbat summit ridge from eastern Toshain Glacier. Local peaks on summit ridge average ~7000m. Nanga Parbat (8143m) is higher, and ~50 NW dipping biotite gneisses are hence clear. Extensive leucogranite (~1.5 km thick) is present on main Rupal Face. Valley in centre left of field of view is Mazeno Glacier valley. Join between Mazeno Glacier abandoned medial moraine and Toshain Glacier lateral moraine is ~4200m. Thrusts are interpreted on Mazeno Glacier valley left bank (1) in saddle partly obscured by shadow, and (2) in saddle (not visible, marked 5639m on map) between snow covered ridge in background and craggy ridge in centre.

Figure 5.54

Figure 5.54 L-tectonite granitic orthogneiss ~200m S of #CR52 on Shaggin Glacier left bank. This type of L-orthogneiss is ubiquitous to the SW Rupal area. Where foliation surfaces are clear, shear fabric is marked by (1) biotite planes forming S and C surfaces. and (2) 0.1-3.0 cm asymmetric feldspar porphyroclasts. Foliation is 031°/70°W with stretching lineation pitching 62° from south. Sense of displacement is top down to SW and sinistral.

Figure 5.55

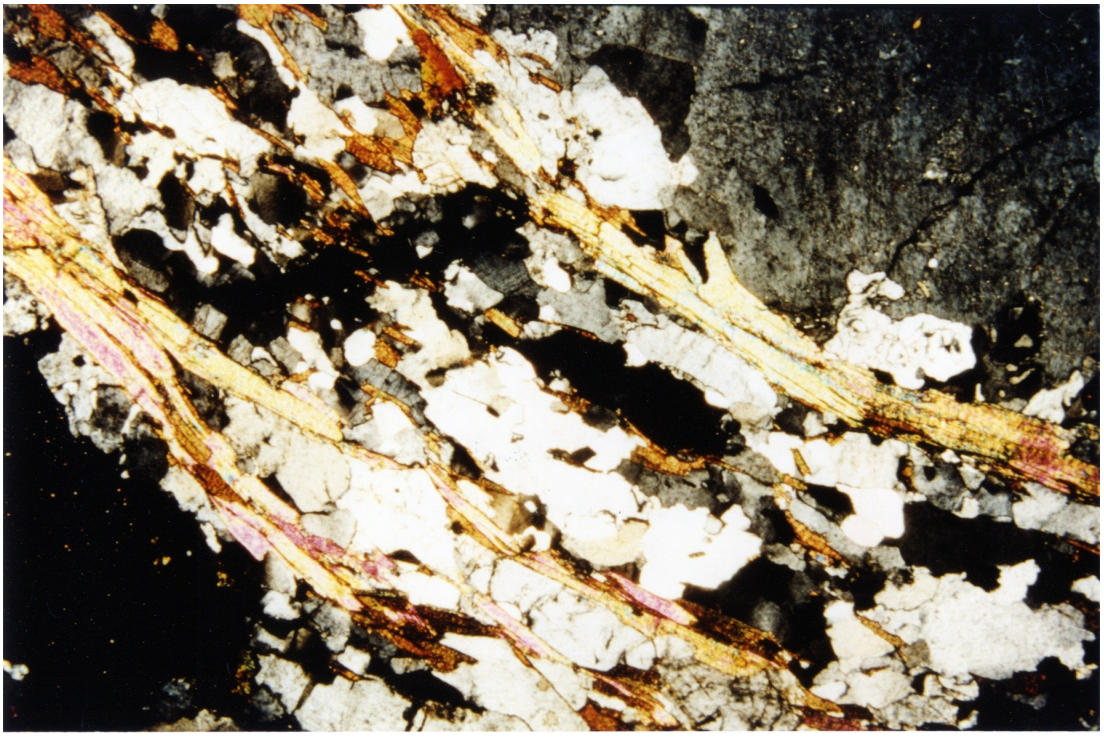

Figure 5.55 Optical photomicrograph of thin section 69-28A (cut from E6/9/28-I sampled near #CR52). Shows characteristic microstructure of L-orthogneiss in SW Rupal. Sense of shear is sinistral, rarely visible at <10 mm width of view due to coarseness of fabric. Sigmoidal feldspar porphyroclasts and 100-400 μm biotite surfaces are main shear indicators. Note overall coarseness of grains. Although some compositional banding is present, quartzofeldspathic bands do not have ribbon-type appearance, and I suggest lattice preferred orientation of biotites is a relict of super-solidus flow, and principal deformation proceeded at <400°C. Cut parallel with lineation (50°-S pitch), perpendicular to foliation (037°/66°E). South is to left. Base of image is 5.5 mm and oblique to main fabric. Crossed polars.

Figure 5.56

Figure 5.56 Granitic orthogneiss on Mazeno Glacier Valley left bank at outcrop #21. Biotite planes mark S and C surfaces. Shear sense is also demonstrated by coarse (<2 cm) feldspar porphyroclasts with asymmetric tails. Foliation is 020°/90°W and stretching lineation plunges 50° towards 020°. Sense of displacement is E side upwards and vergent towards S (dextral shear).

Figure 5.57

Figure 5.57 Photo (looking due east) showing suite of NW dipping pegmatitic sheets ~500-1000 m north of #22, Sheets are discordant to local foliation but, interestingly, are parallel to foliation of country rock (gneiss) at #23, ~1 km across the glacier to the NW, and at Mazeno Pass. Glacier in foreground is ~5000 m. Float includes granitic orthogneiss and various members of compositionally layered gneisses. Green pinninitised cordierite in coarse (pegmatitic) granitoid float was seen in significant volumes, but not in outcrop.

Figure 5.58

Figure 5.58 Looking at east side of Mazeno Pass. Compositionally layered gneiss trending 050°/80°W is clear. Note lack of visibility of Mazeno Pass Pluton from only few 100 m from Pass. Compositionally layered gneisses are cut at high angle by fine grained leucogranite offshoots of Mazeno Pass Pluton (not visible in photo). Pass is 5358 m, top of outcrop to left is ~5400m.

Figure 5.59

Figure 5.59 View directly up steep West face of Mazeno Pass. Viewer is ~300 m below pass (snow covered lower spot to left of picture). Photo clearly shows Mazeno Pass Pluton main body and offshoots cross-cutting country rock (compositionally layered gneisses). Pluton continues for a further 100 m below and a few 100 m to both left and right of field of view.

Figure 5.60A

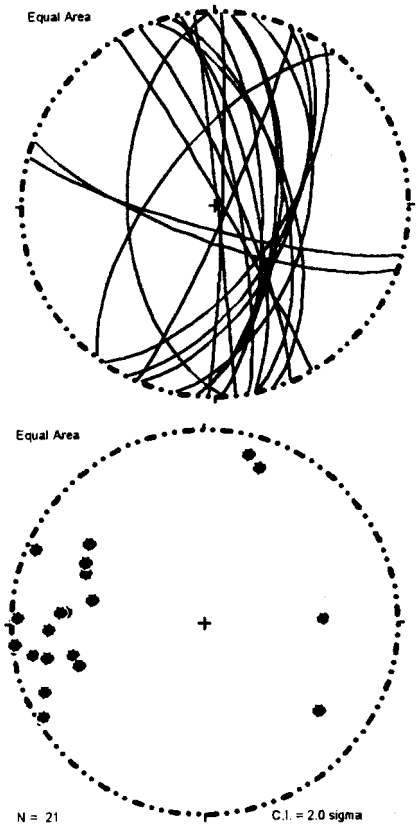

Figure 5.60A Contoured lower hemisphere equal area projection of foliation poles and lineation of all rocks in Diamir Gah.

Figure 5.60B

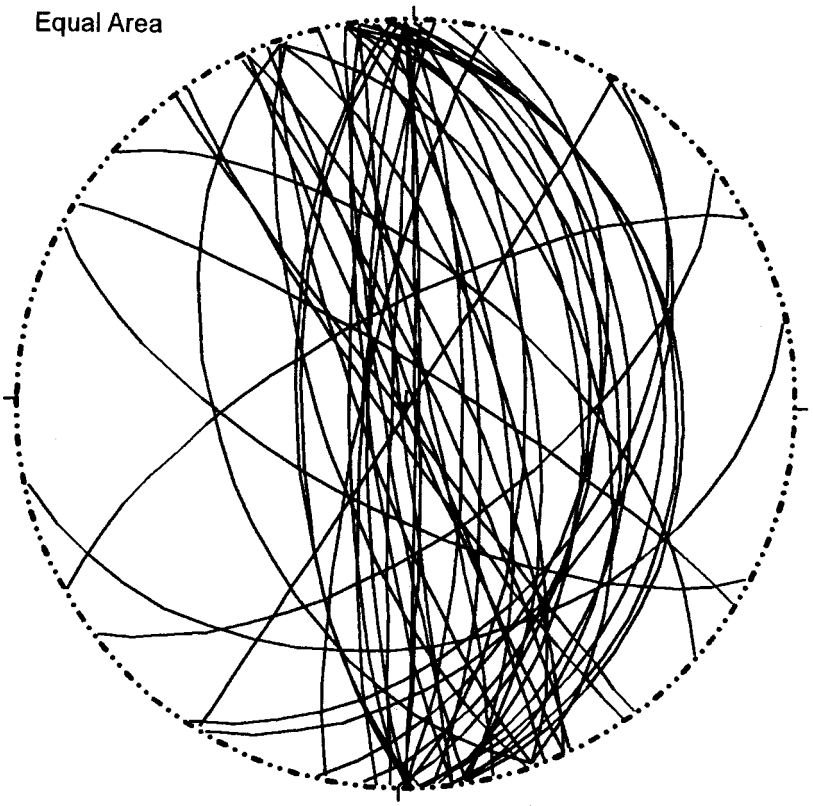

Figure 5.60B Contoured lower hemisphere equal area projection of foliation poles and lineation of all rocks in Airl Gah.

Figure 5.60C

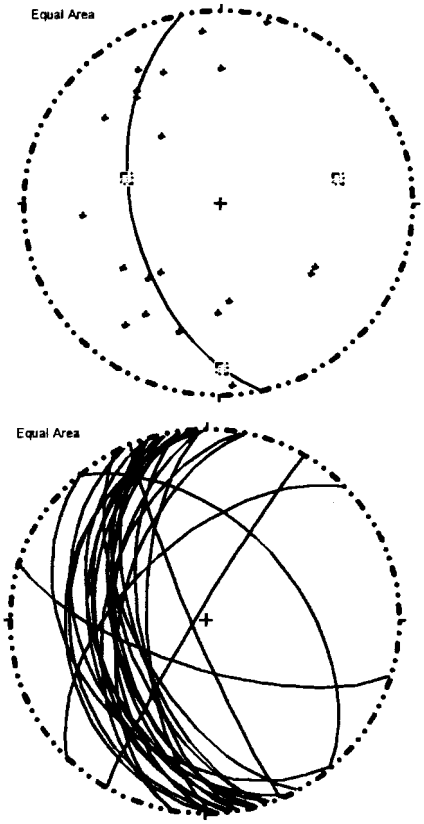

Figure 5.60C Lower hemisphere equal area projection of foliation poles and lineation of all rocks in Biji area. Upper plot: Biji area contoured foliation poles (Kamb method). Lower plot: Biji area contoured lineations (Kamb method).

Figure 5.61A

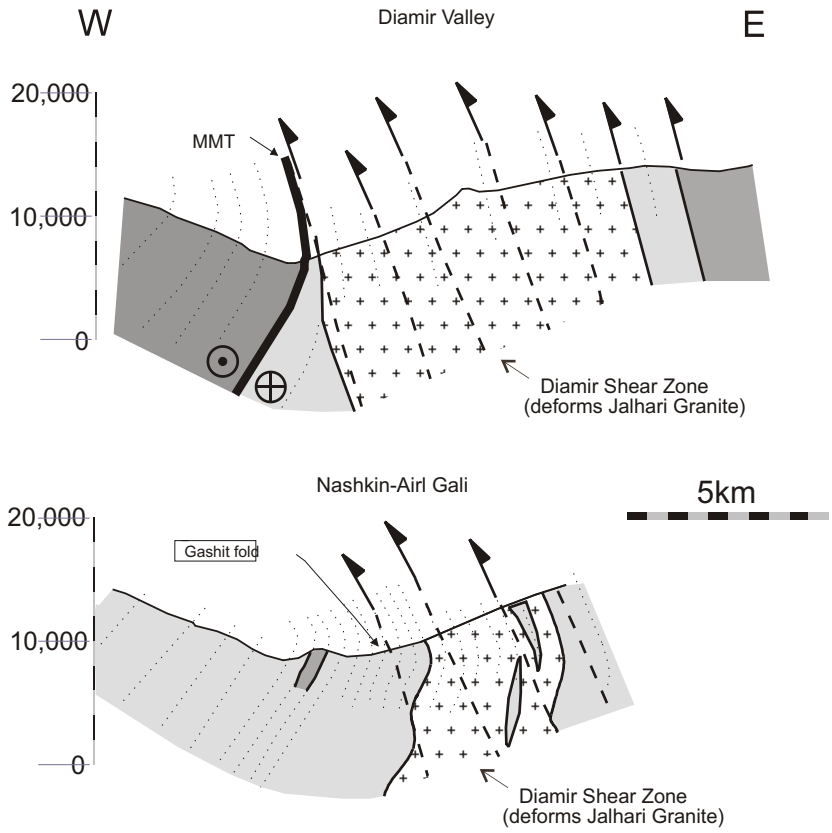

Figure 5.61A Cross sections along Diamir section and Nashkin-Airl composite section. Vertical scale in feet. No vertical exaggeration. Light grey: Metasedimentary cover rocks (dashed line ornament indicates foliation); crosses: leucogranite; medium grey: other gneisses; dark grey: general KLS (only W of MMT). Note overturning of metasedimentary cover rocks in MMT footwall in response to NPHM uplift related overthrusting. Diamir shear zone is primarily focussed in Jalhari granite, emplaced syn-kinematically.

Figure 5.61B

Figure 5.61B View (due W) from Airl Gali pass, looking (1) down Airl Gah, where >5 km of structural thickness of Jalhari granite is represented, (2) past Gashit fold where point of regional overturning of several km of MMT foot-, and hanging wall sequences is accommodated, (3) across Manogush Ridge (in shadow) where belt of porphyroclastic gneiss is present, (4) up into Nashkin Valley, where ~2600m of vertical relief, and >8 km of cover sequence is represented, and (5) to dark rocks of Kamila amphibolite that mark MMT hanging wall at very top of furthest ridge.

Figure 5.62

Figure 5.62 Looking NNW to outcrop of Gashit Fold, on right bank, and towards mouth, of Airl Gah Valley. In this outcrop, fold is within metasedimentary cover, ~1.5 km west of edge of Jalhari Granite. Fold accommodates regional overturning (eastward dip) of MMT footwall, and is inferred to be due to W-verging, E-dipping Airl-Gah/Diamir Shear Zone. North and East of this point, layering is predominantly E-dipping. South & West of this point, layering is predominantly W-dipping (note W-dipping cover rocks in background on far side of Bunar Gah). Hinge line plunges ~ 20°N

Figure 5.63

Figure 5.63 Strained portion of Jalhari granite within Airl-Gah Shear Zone, Diamir Valley: Note large variety of granitic gneiss locally housed. Sample is none the less representative of degree of variation observed throughout Jalhari Granite.

Figure 5.64

Figure 5.64 "Pancake biotite" portion of Jalhari granite within Airl-Gah Shear Zone, Airl Gah (~`500 m W of #AR6). I infer large amounts of super solidus deformation.

Figure 5.65

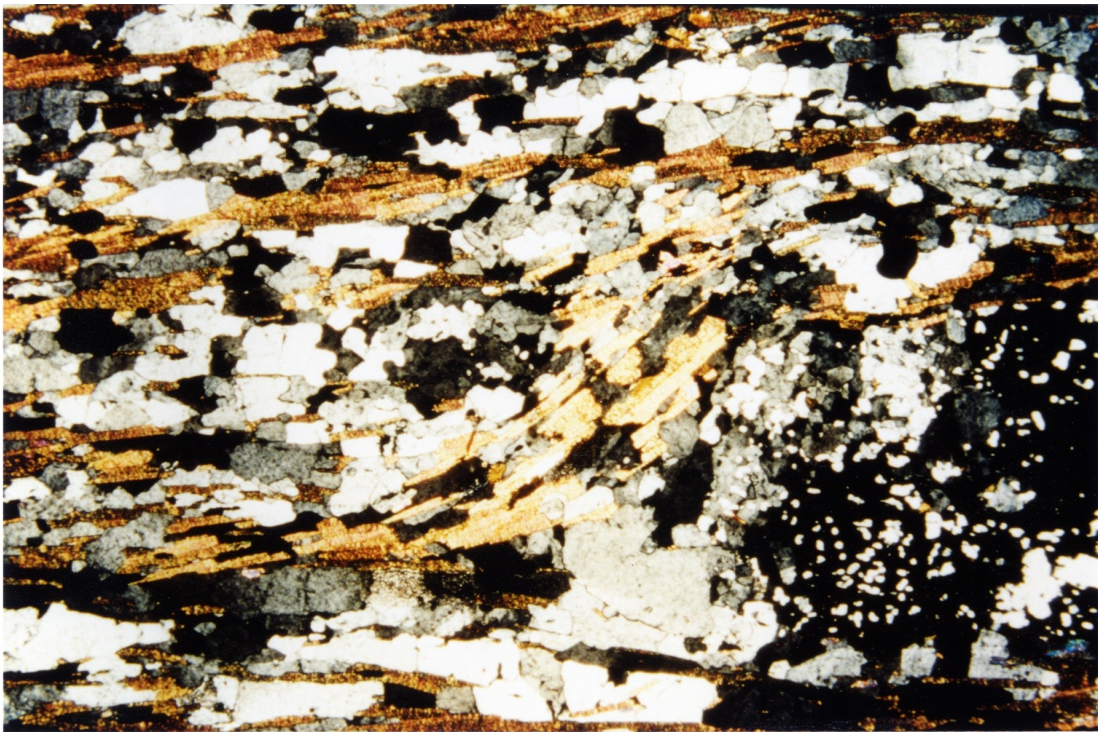

Figure 5.65 Optical photomicrograph of thin section 5-11G cut from NE95-11-VII (not shown). Note the partial development of polymineralic ribbons (see text for discussion). Shows characteristic microstructure of Jalhari granite in Diamir shear zone. Grain size is relatively fine (biotites <300 μm, quartzofeldspathic grains <400 μm). Biotite nicely picks out S and C surfaces. Sense of shear in this case is clearly dextral but note plunge of lineation (50°@350°) i.e., >50% of displacement (in present orientation) is W vergent. Cut parallel with lineation (50°@350°), perpendicular to foliation (170°/89°E). South is to left, west is to top. Base of image is 5.5 mm and parallel with main fabric. Crossed polars.

Figure 5.66

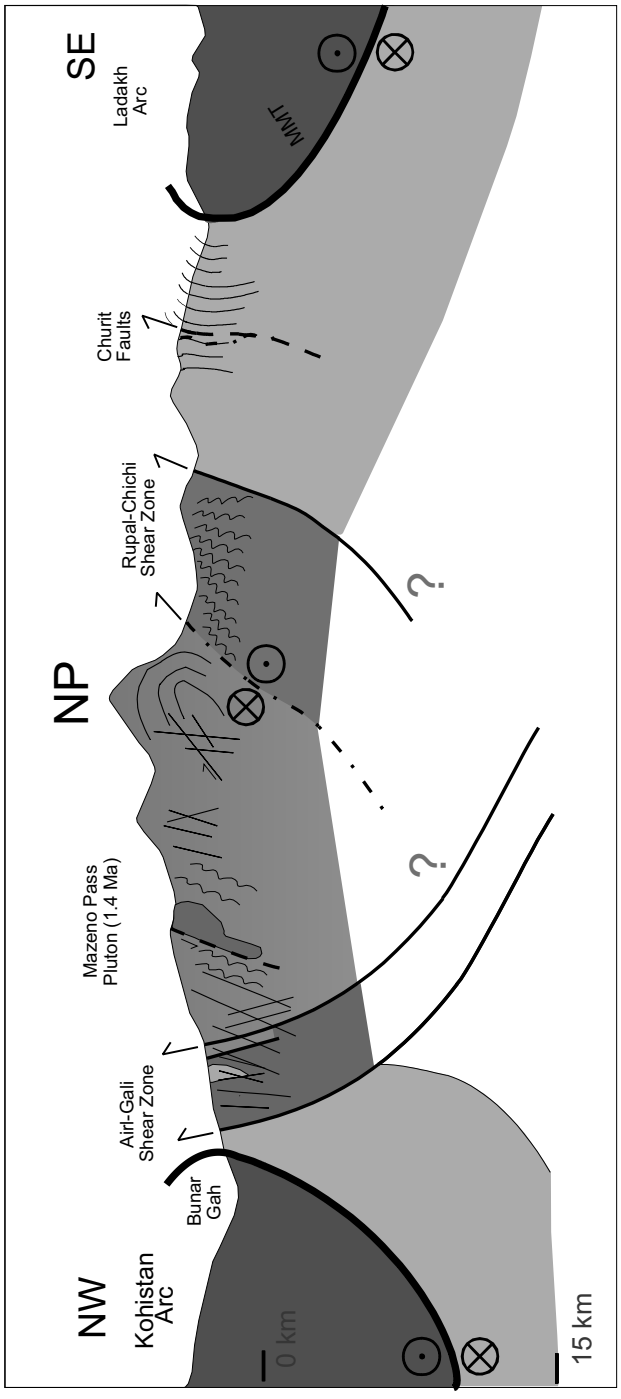

Figure 5.66 Summary cross section for Southern NPHM. Light grey: Metasedimentary cover rocks (dashed line ornament indicates foliation); crosses: leucogranite; medium grey: other gneisses; dark grey: general KLS (structurally above MMT). See text for discussion.